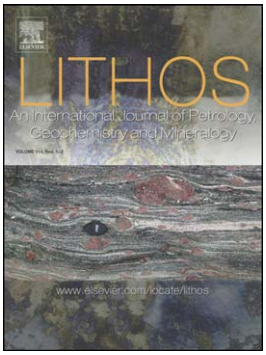

Geochemical and isotopic constraints on island arc, synorogenic, post-orogenic and anorogenic granitoids in the Arabian Shield, Saudi Arabia

F.A. Robinson, J.D. Foden, A.S. Collins

PII: S0024-4937(15)00029-8
DOI: doi: 10.1016/j.lithos.2015.01.021
Reference: LITHOS 3507

To appear in: *LITHOS*

Received date: 22 November 2014
Accepted date: 27 January 2015

Please cite this article as: Robinson, F.A., Foden, J.D., Collins, A.S., Geochemical and isotopic constraints on island arc, synorogenic, post-orogenic and anorogenic granitoids in the Arabian Shield, Saudi Arabia, *LITHOS* (2015), doi: 10.1016/j.lithos.2015.01.021

Geochemical and isotopic constraints on island arc, synorogenic, post-orogenic and anorogenic granitoids in the Arabian Shield, Saudi Arabia

F.A. Robinson[a*], J.D. Foden[a], and A.S. Collins[a]

[a]Department of Earth Sciences, The University of Adelaide, SA, 5005, Australia
*Corresponding author: frank.robinson@adelaide.edu.au, 14 Johnson Road, Athelstone, SA, 5076 Australia Ph +61 0468548502
Co-authors: john.foden@adelaide.edu.au, alan.collins@adelaide.edu.au

The Arabian Shield preserves a protracted magmatic record of repeated amalgamation of juvenile subduction terranes that host granite intrusions ranging in age from the early Neoproterozoic to the Cambrian, which were emplaced into convergent and within-plate settings. Geochronology and whole-rock geochemistry of sampled Saudi Arabian granitoids defines and distinguishes four discrete age groups: 1) ~ 845 – 700 Ma island arc and synorogenic granitoids (IA+Syn), 2) ~ 640 – 610 Ma granitoids from the Nabitah and Halaban Suture (NHSG), 3) ~ 610 – 600 Ma post-orogenic perthitic (hypersolvus) granitoids (POPG), and 4) <600 Ma anorogenic aegirine-bearing perthitic (hypersolvus) granitoids (AAPG). Groups 1, 2 and 3 include suites ranging from I-S- to A-type granites that have REE signatures typical of volcanic arc settings and show intra-suite variation that could be controlled by a combination of crustal assimilation and fractional crystallisation. Their mafic parental magmas have N-MORB-, or arc-tholeiite-like geochemistry. By contrast, group 4 A-type granites are more enriched in HREE and in incompatible elements such as Nb, Rb, Ga, Nd, Zr and Y and have lower Ce/Yb and higher Y/Nb ratios. These granitoids are interpreted to have been emplaced into within-plate and back-arc settings. Granitoid data also provide evidence that there may be two distinct mantle sources to the mafic parents of the granite suites. These are distinguished as contaminated and enriched mantle using Nb and Y and Nd isotopes. All granitoid suites are isotopically juvenile (εNd + 3 to + 6) and fall between the upper field crustal values of the

Paleoproterozoic Khida terrane (εNd + 1) and contemporary depleted mantle. However, Nd isotopes distinguish contamination in group 1-3 mafic end-members beneath sutures which are interpreted to be derived from the contemporary MORB-type mantle wedge with subsequent crustal assimilation and fractionation to I- and A-type granitoids. The youngest (after 600 Ma) A-types (group 4) emplaced into extensional within-plate and back-arc settings require a new enriched mantle source that this study interprets to be associated with delamination.

Keywords: Arabian Shield, island arc, synorogenic, post-orogenic, magmatism, mantle, granite

1. Introduction

Granites are the most abundant rocks in the Earth's upper continental crust. These form in diverse tectonic settings such as convergent plate margins, orogenic belts, oceanic spreading centres and within-plate and back – arc settings, and are often associated with the initiation and termination of supercontinental cycles (Bonin, 2007; Goodge and Vervoort, 2006). An important and widely studied granite group, the A-type granite, is generated in regions of uplift and crustal extension occurring at the termination of orogenic convergence. As indicated by Eby (1990) and Frost et al. (2011), these granites are characterised by high total alkalis, high FeO/FeO+MgO, high REE (including Zr, Nb, Ta) and involve little crustal input. Many studies (e.g. Pearce et al. 1984a; Turner and Foden, 1996; Turner et al. 1992) favour fractionation from enriched mantle derived basalts with only limited crustal contamination.

However, alternative studies (e.g. Kerr and Fryer, 1993; Han et al. 1997) also indicate the derivation of A-types from the depleted mantle with minor crustal assimilation.

The complex interplay of early Neoproterozoic to Cambrian granitoids associated with the closure and accretion of juvenile volcanic arcs and back-arc basins in the Arabian-Nubian Shield (ANS) provide an ideal setting to examine a diverse range of magmatic sources. Johnson et al. (2011) describe the tectonic timing and East African Orogen significance of the pre 650 Ma and late Cryogenian-Ediacaran (650 − 542 Ma) magmatism in the ANS, but indicate that the geochemical aspects require further study. One of the most abundant and debated ANS intrusives are the post-collisional A-type granites that are variously argued to be derived from either isotopically juvenile but enriched mantle or from depleted mantle (Be'eri-Shlevin et al. 2010; Stein and Goldstein, 1996; Stoeser and Frost, 2006). Recent studies in Sinai (Azer and Farahat, 2011; Eyal et al. 2010) follow the work of Brown et al. (1984) and Bonin (2004) and suggest two distinct mantle sources involved in the transition from post-collisional calc-alkaline to anorogenic alkaline granitoids. To account for this transition and widespread voluminous magmatism following Gondwana amalgamation, their petrogenesis is often attributed to slab roll-back (Flowerdew et al. 2013) and/or lithospheric delamination (Avigad and Gvirtzman, 2009). Alternatively, Stein and Goldstein (1996) suggest an enriched mantle plume (± crustal overprinting) that can be geochemically traced to ~1000 – 650 Ma oceanic tholeiites and bimodal volcanism sequences in intra-oceanic settings.

This work focuses on the Saudi Arabian part of the ANS and presents the geochemical properties of the island arc (~845 Ma), synorogenic (~715 – 700 Ma),

post-orogenic (~640 – 600 Ma) and anorogenic (~600 Ma) granitoids published in Robinson et al. (2014). These four groups are defined by granitoid U-Pb age and structural/petrographic observations described in Robinson et al. (2014) combined with geological maps and interpretations from Johnson (2006) and Johnson et al. (2011). Following the studies from Stein and Goldstein (1996), Stoeser and Frost (2006) and Be'eri-Shlevin et al. (2010), new whole-rock and Nd-Sr isotope geochemical data from the four granitoid groups covering all but the Ar Rayn Terrane and majority of the Asir Terrane (exception northern and eastern side), will aim to examine the arguably enriched or depleted mantle involved in generating juvenile Saudi Arabian granitoids. Similar to studies in Sinai (Azer and Farahat, 2011; Eyal et al. 2010), particular emphasis will be placed on the post-orogenic and anorogenic phases, which according to Robinson et al. (2014), indicate a change in tectonic process.

2. Arabian Shield Geological Setting

The Arabian Shield forms a series of tectonostratigraphic terranes composed of geochemically diverse early Neoproterozoic to Cambrian (~850 − 525 Ma) granitoids intruding volcanosedimentary basin assemblages. With a general younging towards the east (Stoeser and Camp 1985; Stoeser and Frost, 2006; Johnson et al., 2011; Stern et al. 2010), the Shield is composed of eight isotopically and geochronologically discrete terranes separated by five ophiolite-bearing suture zones. Stoeser and Frost (2006) indicate that the Arabian Shield structure consists of two parts: the western side comprising the Midyan, Hijaz, Jiddah and Asir island arc terranes which are of oceanic arc affinity; and the eastern side composed of the

Tathlith, Ha'il, Afif, Ad Dawadimi, and Ar Rayn Terranes which are also of oceanic arc affinity (**Figure 1**). However, they single out the Khida sub-terrane (southern Afif Terrane) that is composed of pre-Neoproterozoic continental crust and indicate that the mantle source associated with the western terranes is more depleted than the eastern terranes and/or the eastern terrane mantle source has incorporated a small crustal component. According to Johnson et al. (2011), both western and eastern terranes have been deformed by at least four periods of arc collision and suturing, and are overlain and intruded by post-amalgamation (<640 Ma) basins (e.g. Nettle et al. 2014) and granitoids. The amalgamated terranes have been affected by multiple exhumation and erosion events. A Cambrian regional unconformity post-dates the youngest plutons, recently dated at <525 Ma (Robinson et al. 2014).

The Arabian Shield preserves a series of discrete Neoproterozoic tectonomagmatic events initially defined and described by Bentor (1985) and later Stein and Goldstein (1996). In general, the earliest (~950 − 650 Ma) oceanic tholeiite and bimodal volcanism is confined to the western Arabian Shield, has island arc chemistry and is emplaced in intra-oceanic settings. The younger phases cover vast

(**insert Figure 1**).

areas of the western and eastern Arabian Shield and are dominated by 640 − 590 Ma calc-alkaline batholiths terminating with a strong uplift and a switch to 590 − 550 Ma alkaline granites and volcanics (Black and Liegeois, 1993). The ~780 − 600 Ma collision of the Yanbu and B'ir Umq Sutures in the west and the Nabitah and Halaban Sutures in the east was magmatically the most productive, resulting in extensive

north-south trending granitoids in subduction and back-arc environments. The N-S trending Nabitah Belt forms arguably the most significant part of this magmatic history and is interpreted to result from collision between western island arcs and the eastern Afif terrane that is floored with pre-Neoproterozoic continental crust (Stoeser and Camp, 1985; Stoeser and Frost, 2006; Stern et al. 2010). This suture consists of deformed volcanic/pre-collision basins intruded by post-collision granitoids/basins and according to Johnson et al. (2011), the Nabitah collision was not synchronous, but initiated at ~680 Ma in the north (Midyan, - Hijaz and -Afif Terranes), while subduction continued in the south (Asir, - Tathlith and -Afif Terranes). Recent studies conducted by Flowerdew et al. (2013) demonstrated that the Nabitah Belt separates juvenile Neoproterozoic intra-oceanic arc terranes and propose that plutons confined to its southern end, form as a consequence of subduction slab roll-back. It is speculated that the terranes either side of the Nabitah Belt were sutured by ~640 Ma, but further east in the Ar Rayn and Ad Dawadimi Terranes, subduction continued until after ~600 Ma (Cox et al. 2012; Doebrich et al. 2007).

Recent Arabian Shield geochronological data from Robinson et al. (2014) distinguished island arc (845 Ma), syncollisional (~715 – 710 Ma), post-orogenic (~640 – 600 Ma) and anorogenic (<600 Ma) magmatism from 20 plutons spread across 8 terranes (**Figure 1**). These cycles represent different tectonic processes in the Shield evolution and produced a diverse range in plutonic mineralogy. A petrographic representation of each tectonic cycle is displayed in **Figure 2**. Petrographic details for each of the 20 suites are described in Robinson (2014) and are summarised in **Table 1**. The island arc age samples correspond with the Makkah Suite (Jiddah Terrane), which consists of subrectangular plutons composed of predominantly granodiorite-

tonalite cross-cut by gabbro-dioritic and rhyolitic dykes. Further north, cross-cutting the Yanbu Suture (Hijaz terrane), are synorogenic suites that form irregular shaped batholiths composed of granodiorite/tonalite. Separating the island arc/synorogenic western Arabian Shield and the post-orogenic eastern Arabian Shield

(**insert Figure 2**).

with abundant hypersolvus granitoids, is the Nabitah Suture. This hosts undeformed intrusions ranging from gabbros and diorites to granites and aegirine perthitic alkali-granites. The younger anorogenic suites are spread over both the western and eastern Shield and form undeformed, rounded, ring-shaped plutons with aegirine-bearing alkali-granite mineralogy. Taking this into account, this study will maintain the island arc, synorogenic, post-orogenic and anorogenic phases defined by Robinson et al. (2014) and use these as a systematic way to present geochemistry from 137 samples. The assigned tectonic grouping of the 20 sampled suites is displayed in **Table 1**.

3. Analytical Techniques

Detailed analytical procedures for major and trace element, REE and Nd-Sm-Sr isotope geochemistry are described in **Appendix C**. Standard reference geochemistry is presented in **Appendix A**.

3.1. Major and Trace Element Chemistry

All 137 samples collected in the Arabian Shield were cleaned of weathered material and a fraction was then ring milled between tungsten carbide plates. Both major and trace element analysis was performed at the University of Adelaide using a Phillips PW1480 X-ray spectrometer. Major elements were analysed using the Sc-Mo tube operated at 40kV-75mA with values expressed as oxides and the total iron content. The program was calibrated against international and internal standard reference materials BHVO-1/BCR-1 (USGS) and TASBAS (Adelaide University). Trace elements used both the Sc-Mo tube (higher voltages) and the Au tube operated at 50kV, 40mA. However, several calibration programs were used with up to 30 standard reference materials. Matrix corrections were made using either the Compton scatter peak, or mass absorption coefficients calculated from the major element data. These results are presented as parts per million (ppm) with the calibration assuming levels of 1-2000 ppm. Negative values generated by interference and X-ray detection limit are presented as zero values. The assigned XRF Fe_2O_3 (Total) values were further separated into ferrous (FeO) iron content through a wet chemical procedure described in Sossi et al. (2012). To gauge procedure reliability an internal standard TASBAS (12.71wt% Fe_2O_3T) was analysed prior to, intermittently, and at the termination of unknown samples. A total of 30 TASBAS standards were measured, producing an average of 9.34 wt% FeO and 2.33 wt% Fe_2O_3. The reproducibility of the internal standard renders the Arabian data confidently reliable.

3.2. Rare Earth Element (REE) Geochemistry

A nominal 100mg of milled sample was accurately weighed into clean Teflon bombs and digested in a series of distilled 50% HF and 7M HNO_3^- acids using heated

pressure vessels. Sample solutions were analysed at Adelaide Microscopy using an Agilent 7500 solution inductively coupled mass spectrometer (ICPMS). Calibration was achieved by external standardisation with signal intensities of all isotopes measured in blank as well as artificial solution concentrations. This was determined prior to analysis and repeated on termination, which established a calibration curve. Element raw counts per second were converted to concentration (ppb) through fitting the unknown data to the calibration curve. Instrument drift and matrix effects were corrected by using a ^{103}Rh-^{115}In solution. These non-interfered, mono-isotopic isotopes are used as the internal standardisation and corrections are applied to the raw counts per second of the unknown sample. Procedural blanks and standard reference material G-2, GPS-2 and BCR2 (USGS) were also prepared to gauge procedure and machine accuracy. Unknown sample concentrations were cross-referenced with XRF data to determine reliability. Standard reference materials are within acceptable error of the USGS values.

3.3. Neodymium (Nd) and Strontium (Sr) Isotope Geochemistry

Twenty suites that had previously been dated and analysed for Hf isotopes (Robinson, et al. 2014) were selected for Nd-Sm and Sr isotopic analysis. The samples chosen are thought to adequately represent their respective suite. An additional 10 country rocks and gabbroic autoliths were also analysed. Nd-Sm and Sr isotopes were measured at the University of Adelaide using a Finnigan MAT262 thermal ionisation mass spectrometer (TIMS). Procedural blanks (n=4), international and internal standards (G-2 n=3, JNdi1 n=7 and SRM987 n=9) were analysed prior to sample analysis to gauge machine accuracy and precision. Procedural blanks

registered <100pg Nd, <20pg Sm and <850pg Sr, thus showed negligible contamination or procedural error. International standards G-2 (USGS Nd μgg^{-1} = 55 [±6], University of Adelaide G2 Sm/Nd spike F = 51.2 [±3.9] – n=11) and JNdi (Tanaka et al. 2000 = 0.512115 [±7], University of Adelaide = 0.512085 [±9.5] - n=650) produced Nd values of 52.6 μgg^{-1} and 0.512082 [±8.7] respectively. Internal standards SRM9878 (University of Adelaide $^{87}Sr/^{86}Sr$ = 0.710268 [±17.2] – n=744) and G2 (USGS $^{87}Sr/^{86}Sr$ =0.709770 [±7], University of Adelaide $^{87}Sr/^{86}Sr$ =0.709741 – n=11) produced $^{87}Sr/^{86}Sr$ values of 710233 [±11.9] and 0.709738 [±12] respectively. Overall, the analysed standards are within accepted values, hence the Arabian samples are deemed reliable.

Present day εNd values were obtained using $^{143}Nd/^{144}Nd$ CHUR (0.512638), $^{147}Sm/^{144}Nd$ (0.1966), $^{143}Nd/^{144}Nd$ DM (0.513150) and $^{147}Sm/^{144}Nd$ DM (0.2145) ratios taken from Goldstein et al (1984). Depleted Mantle model ages (T_{DM}) are calculated based on these ratio values. Granitic components are assigned ages that have been directly dated using U-Pb zircon geochronology (Robinson et al. 2014). Although not directly dated, parent gabbroic autoliths are assumed to be the same age as the granitic product in the same suite. All remaining suites not directly dated are assigned published age values obtained from Johnson (2006).

4. Results

4.1. Major and Trace Element Geochemistry

Whole-rock geochemistry results are summarised in **Table 2** and granitic classification and tectonic discrimination in **Table 3**. Raw geochemical data and values marked with an * are presented in supplementary **Appendix A**.

The island arc and synorogenic (IA+Syn) granitoids range from tonalites (~65 wt%) to granodiorites (~73 wt%) with amongst the highest CaO (~2 – 4 wt%), MgO (~0.5 – 2 wt%) and lowest total alkalis (~6.2* – 6.7* wt%) of all sampled Shield suites (**Figure 3).** Other distinguishing features include low-moderate TiO_2 (~0.2 – 0.7 wt%), high Mg# (~0.2* – 0.4*) and amongst the lowest Nb (~3 – 8 ppm), Rb (~26 – 43 ppm), U (~0.1* – 2* ppm), Zr (~131 – 336 ppm), Nd (~13* – 26 ppm), La (<15 ppm) and Y (~18* – 50 ppm) of any sampled suites. IA+Syn suites are I-type granites that are classified as magnesian (~0.6 – 0.7), calcic/calc-alkalic and metaluminous (**Figure 4**). They are also confined to the VAG tectonic field (**Figure 4**). These suites have both LREE enrichment (particularly Rb, Ba, K and U) and middle REE enrichment, but HREE concentrations similar to N-MORB (**Figure 5**). They also possess strong negative Nb anomalies and minor negative Eu and positive Sr anomalies which are indicative of feldspar fractionation.

(**insert Figure 3**).

Post-orogenic granitoids range from quartz-monzonites (~64 – 68 wt% SiO_2) to alkali-granites (~70* – 76 wt% SiO_2) characterised by the largest range of TiO_2 (~0.05* – 0.8 wt%), Mg# (~0.03* – 0.56*), CaO (~0.3* – 2.7* wt%) and Al_2O_3

(~10.8* – 17.9* wt%) of any magmatic group (**Figure 3**). They also have amongst the highest Fe# (~0.18* – 0.97*) and total alkalis (~7.3* – 9.7* wt%), and are distinguished by compositional trends initiating near MORB and extending into the anorogenic field (**Figure 3**) . Similarly, the trace elements also have a large range and include Nb (~5 – 51* ppm), Rb (~61 – 240* ppm), U (~1* – 13 ppm), Nd (~8* – 115 ppm) La (~7* – 140) and Y (~9* – 227* ppm), which are amongst the lowest and highest sampled in the Shield. Post-orogenic granitoids are both I- and A-type granites that illustrate a transition from magnesian (~0.2 – 0.7) to distinctly ferroan (>0.7 – 0.9) end-members (**Figure 4**). This transition trend continues with intermediate samples classified as metaluminous, calcic/calc-alkalic and VAG, whilst more felsic

(**insert Figure 4**).

components are classified as peraluminous-peralkaline, alkali/alkali-calcic and WPG (**Figure 4**). This group also has the most diverse REE patterns of all magmatic groups. The most primitive are enriched in LREE, but are more depleted in HREE than N-MORB, and contain strong negative Nb, Sr, Zr, Nd and Y anomalies (**Figure 5**). Felsic end-members are also enriched in LREE, but are notably more enriched in HREE (~100 times more enriched). These contain similar anomalies, but also negative Eu indicative of feldspar fractionation.

(**insert Table 3**).

Anorogenic granitoids range from syenites (~60 – 61 wt%) to granites and alkali-granites (~71 – 78* wt%) that are amongst the most iron-rich (~0.47* – 0.89* Fe#) and alkali-rich (~8.2* – 11.2* wt%) suites sampled in the Arabian Shield. They also have a large range in TiO_2 (~0.01* – 0.98* wt%), Al_2O_3 (~10.1* – 18.6* wt%) and CaO (~0.25* – 3.2* wt%) and predominantly cluster in the silica range of 70–80 wt% (**Figure 3**). Similarly, they have a large range in Nb (~1* – 77* ppm), Rb (~41 – 332* ppm), U (~1 – 21* ppm), Nd (~4* – 127 ppm) and La (~1* – 155) in which the highest values are the highest sampled in the Shield. It should be noted that the garnet-bearing Malik Granite consistently forms the lowest values, which dramatically skews the concentration range. Anorogenic granitoids are classified as S- (Malik Granite), borderline I- (Admar Suite) and A-type granites (**Figure 4**). They are also predominantly ferroan (~0.8), but the Al Bad suite (~76 wt% SiO_2) and Malik Granite contain both magnesian (~0.1 – 0.4) and ferroan (~0.8) components, which may be attributed to mineral heterogeneity between samples (**Figure 4**). Anorogenic granitoids are also predominantly peraluminous and calc-alkalic/alkali-calcic, but syenitic suites are metaluminous and strongly alkalic (**Figure 4**). Similarly, most are confined to the WPG tectonic, but the Malik Granite and Admar Syenite are classified as VAG suites (**Figure 4**). Anorogenic suites also produce diverse range in REE patterns. These have similar LREE, middle REE and HREE enrichment patterns to post-orogenic suites and also contain the negative Sr, Eu, P, Ti anomalies attributed to feldspar fractionation (**Figure 5**). However, they are notably less depleted in HREE signatures compared to post-orogenic suites.

(**insert Figure 5**).

4.1.1 Arabian Shield Mafic Intrusives

Island arc (Makkah Suite), post-orogenic (Al Hafoor and Kawr Suites) and anorogenic (Rithmah Complex) groups contain gabbroic end-members predominantly composed of plagioclase, pyroxene, amphiboles, hornblende and olivine. Island arc gabbro-diorites (~52* – 54 wt% SiO_2) are characterised by high total alkalis (~4* – 5* wt%), TiO_2 (~1.2* –1.3 wt%), Fe_2O_3T (~9.5*–10.8* wt%) and low Al_2O_3 (~15.5–16* wt%) compared to other Shield gabbroic components. They also have moderate Cr (~65* – 110* ppm), Y (~30–32* ppm), Zr (~97* – 110 ppm) and Nb (~2*–6 ppm), which classify these as MORB/N-MORB mafic components (**Figure 6**). By contrast, post-orogenic gabbros and diorites (~44* – 57* wt% SiO_2) have the largest compositional range that results in the lowest and highest CaO (~4.7* – 16.4 wt%), Al_2O_3 (~13.9* – 25.3* wt%), TiO_2 (~0.06* – 1.8* wt%), total alkalis (~0.6 – 6.4* wt%) and Mg# (~0.38* – 0.84*) compared to other sampled mafic intrusives. Similarly, post-orogenic gabbros and diorites have a large range in Cr (~45* – 321* ppm), Y (~0.3* – 56* ppm), Zr (~4* – 187* ppm) and Nb (~0.1*–21* ppm). As illustrated in **Figure 6**, this compositional range results in Cr rich IAT/N-MORB components (Al Hafoor Suite) and both Y rich and Cr rich MORB and IAT/N-MORB, P-MORB, within-plate tholeiite end-members (Kawr Suite). The dilution of Y observed in the Kawr Suite is attributed to the accumulative mineralogy. Anorogenic gabbro-diorites (~54 – 57* wt% SiO_2) are characterised by low CaO (~7.2*–7.4 wt%), total alkalis (~3.9* wt%) and Mg# (~0.4*) compared to other sampled gabbros. They also contain low Cr (~66*–109* ppm), Y (~14–16* ppm), Zr (~51 – 62* ppm) and Nb (~2* – 3* ppm), which classify these as IAT/N-MORB end-members (**Figure 6**).

(**insert Figure 6**).

4.2. Nd-Sm and Sr Isotopes

Nd-Sm and Sr isotope analyses are summarised in **Table 4** and raw data are presented in supplementary **Appendix B**. Post-orogenic (ao, wb, nr, id) and anorogenic (aa) perthitic granitoids contain high Rb/Sr ratios and have experienced Sr loss (shallow level decompression open system unmixing). Consequently, this causes unreliable initial Sr values for these suites and they are not used in this study.

The island arc gabbro and synorogenic granitoids have amongst the lowest Sm (3.2 – 5. 4 ppm) and Nd (16.3 – 24.7 ppm) concentrations and amongst the highest measured $^{147}Sm/^{144}Nd$ (0.1186 – 0.1353) and $^{143}Nd/^{144}Nd$ (0.512582 – 0.512653) ratios of any granitoids sampled in the Shield. Similarly, the Sr (207.8 – 826.3 ppm) concentrations are amongst the highest, whilst the measured $^{87}Sr/^{86}Sr$ ratios (0.704364 – 0.706177) are amongst the lowest of all granitoids. The calculated εNd (t) values range from + 5.84 to + 5.94 and the corresponding TDM model ages from 0.90 – 1.05 Ga respectively. The calculated initial $^{143}Nd/^{144}Nd$ (0.511852 – 0.512043) and $^{87}Sr/^{86}Sr$ (0.702826 – 0.703102) ratios are amongst the lowest of all samples. **Figure 7** illustrates the juvenile nature of both island arc and synorogenic groups, which form the most juvenile samples in the decreasing juvenility trend of εNd (t) vs. εHf (t).

Post-orogenic granitoid samples contain amongst the lowest and highest Sm (1.7 – 22.5 ppm) and Nd (11.1 – 126.9 ppm) concentrations and measured $^{147}Sm/^{144}Nd$ (0.0791 – 0.1506) and $^{143}Nd/^{144}Nd$ (0.512340 – 0.512630) ratios of all

granitoid groups. This is also consistent with Sr (21.9 – 1024 ppm) values and the highest measured $^{87}Sr/^{86}Sr$ (0.704789 – 0.806404) ratios. The calculated εNd (t)

(**insert Table 4**).

values range from + 1.81 to + 4.99, the TDM model ages from 0.83 – 1.24 Ga and the calculated initial $^{143}Nd/^{144}Nd$ and $^{87}Sr/^{86}Sr$ ratios from 0.511957 – 0.512100 and 0.701513 – 0.753914 respectively. Post-orogenic gabbroic units (ao88 & kw43) have amongst the lowest Sm (1.8 – 5.7) and Nd (7.7 – 25.7 ppm) concentrations and measured $^{147}Sm/^{144}Nd$ (0.1350 – 0.1384) and $^{143}Nd/^{144}Nd$ (0.512477 – 0.512530) ratios of all sampled suites. They also contain high Sr ranging from 235.3 – 454.7 ppm and low measured $^{87}Sr/^{86}Sr$ ratios ranging from 0.704720 – 0.705530. The calculated εNd (t) values are amongst the least juvenile ranging from + 1.68 to + 2.63 and the TDM model ages are amongst the oldest ranging from 1.24 – 1.29 Ga. The calculated $^{143}Nd/^{144}Nd$ (t) ratios are also low ranging from 0.511935 - 0.511953, whilst $^{87}Sr/^{86}Sr$ (t) ratios are high ranging from 0.703831 - 0.705447. As illustrated in **Figure 7**, post-orogenic granitoids are closely associated with juvenile mantle defined by anorogenic A-types. However, the Al Khushaymiyah Suite (Afif Terrane), Ar Ruwaydah Suite (Halaban Suture) and the post-orogenic gabbros, all reside in Khida Terrane field constructed using granitic isotopes taken from Stoeser and Frost (2006).

(**insert Figure 7**).

The anorogenic gabbro and granitoids have the lowest and highest Sm (2 – 21.1 ppm), Nd (7.7 – 138.6 ppm) and measured $^{147}Sm/^{144}Nd$ (0.0873 – 0.1615) and $^{143}Nd/^{144}Nd$ (0.512428 – 0.512790) ratios of all sampled suites. This is similar with Sr concentrations ranging from 9.3 – 570.6 ppm and measured $^{87}Sr/^{86}Sr$ ratios range from 0.703946 – 1.089832. The calculated εNd (t) values range from + 2.33 to + 5.67, which are among the most juvenile of all granites. TDM model ages are on the lower end and range from 0.85 – 1.18 Ga, whilst the calculated initial $^{143}Nd/^{144}Nd$ (0.511984

– 0.512156) and $^{87}Sr/^{86}Sr$ (0.700113 – 0.702819) ratios are amongst the highest and lowest of all sampled granitoids respectively. As illustrated in **Figure 7**, most anorogenic components define a juvenile cluster at ~600 Ma, whilst the garnet-bearing leucogranite (S-type granite) is associated with the Khida Terrane field.

5. Discussion

Following the geochemical subdivision of pre-, syn-, late- and post-collisional granitoids by Harris et al. (1986b), geochronological data from Robinson et al. (2014), combined with the presented geochemical data in this study, defines and distinguishes four discrete age groups: island arc (~845 Ma), synorogenic (~715– 700 Ma), post-orogenic (~640 – 600 Ma) and anorogenic (<600 Ma). As illustrated in **Figure 8**, these granitoids are emplaced into a diverse range of collisional and extensional environments across the Shield. Taking into account the geochemistry and change in tectonic process at ~600 Ma suggested by Robinson et al. (2014), mineralogical and spatial distribution reveals a further subdivision could be introduced: **1)** island arc + synorogenic granitoids (IA+Syn), **2)** post-orogenic perthitic (hypersolvus)/aegirine-bearing granitoids confined to the Nabitah and Halaban Sutures (NHSG), **3)** post-orogenic perthitic (hypersolvus) granitoids (POPG), and **4)** anorogenic aegirine-bearing perthitic (hypersolvus) granitoids (AAPG). These are summarised in **Table 5** and are used throughout this discussion. Given this new identification, the geochemical significance will be discussed first, followed by potential petrogenesis and finally, regional implications for the ANS.

(**insert Table 5**).

5.1. Geochemical discrimination of Arabian Shield granitoids

Sampled Saudi Arabian granitoids are isotopically juvenile (εNd +3 to +6) and fall between the upper field crustal values of the Paleoproterozoic Khida Terrane (εNd +1) and contemporary depleted mantle, but have distinctive geochemical signatures that suggest the involvement of two distinct mantle sources to the mafic parents of the granitic suites. This is emphasised in **Figure 9** by using Nb and Y to suggest two mantle types: **1)** Contaminated Mantle (CM) granitoids; and **2**) Enriched Mantle (EM) granitoids. These two elements are widely accepted and used to discriminate I-, S- and A-type granites and VAG and WPG tectonic process (Frost et al. 2011; Pearce et al. 1984a; Whalen et al. 1989). When applied to the Arabian Shield, Nb and Y clearly distinguish the older (>600 Ma) I- and A-type granites associated with contamination from the younger (<600 Ma) A-types associated with HREE enrichment and limited-crust-mantle interaction, hence the basis for the two mantle types. The identification of two Arabian Shield mantle types is in agreement with Harris et al. (1986a) who discuss post-collisional contaminated (572 Ma) and enriched (534 Ma) sources from the Jabel Sayid Complex . As illustrated in **Figure 9**, the classification of CM and EM granitoids outlines a distinct linear trend of CM defined by IA+Syn, NHSG and POPG suites and a separate EM source associated with the AAPG. IA+Syn, NHSG and POPG suites range from I-, S- to A-type granites, possess REE signatures typical of volcanic arc settings (Rb, Ba, K, U enrichment and negative Nb anomalies), mafic parents with MORB- and arc-tholeiite-like chemistry and show intra-suite variation that could be controlled by a combination of crustal assimilation and fractional crystallisation. Isotopic signatures presented in **Figure 10** indicate that IA+Syn (dm) and NHSG (kw, ao) gabbros alongside side POPG samples (ky), are the least juvenile

(**insert Figure 8**).

of all Arabian samples and are incorporated into the Paleoproterozoic Khida Terrane constructed from granites taken from Stoeser and Frost (2006). It is not suggested that IA+Syn, NHSG and POPG suites are directly derived from this terrane, but rather that they contain a crustal component contaminating the MORB/arc-tholeiite-like mantle in which they are derived. By contrast, EM A-types are distinctly more enriched in HREE and in incompatible elements such as Nb, Rb, Ga, Nd, Zr, and Y. They also have a subtle shift towards higher Nd values (isotopically most juvenile), which possibly indicates a reduction in crustal involvement.

(**insert Figure 9**).

Following the identification of the linear CM trend, it is felt necessary to determine whether fractionation is the dominant process following contamination of MORB-/arc-tholeiite-like mantle. As illustrated **Figure 10**, trends using Ce/Yb vs. Y/Nb indicate that CM granitoids appear to be driven by fractional crystallisation. The CM gabbros contain amongst the lowest Ce/Yb (~10 – 20) and Y/Nb (~2 – 7) ratios and fractionate to granitoids with the highest Ce/Yb (~70 – 120) and Y/Nb (~1 – 3) ratios of all samples. EM suites are clearly isolated with amongst the lowest Ce/Yb (~5 – 50) and Y/Nb (~0.5 – 2) ratios, suggesting they are not the end products of intense fractionation, but rather a differing mantle source. This is further highlighted when utilising SiO_2 and Mg# as an index of fractionation (**Figure 10**). The suggested highly fractionated nature of these post-orogenic CM granitoids is in agreement with Moufti et al. (2013), who indicate that post-collisional (~620 Ma)

suites in the southern Arabian Shield mark the beginning of highly fractionated (alkaline to calc-alkaline) A-type magmatism associated with extension.

(**insert Figure 10**).

5.2. Petrogenesis of Arabian Shield contaminated and enriched mantle

One of the difficulties in distinguishing CM A-type and EM A-type suites is that they contain similar mineralogy, ferroan classification and are associated with extension. However, as illustrated in **Figure 11**, CM A-type suites exhibit a transition from magnesian – ferroan and VAG – WPG classifications. Their mafic parental magmas also have an N-MORB like geochemistry that fractionate to I- and A-type granites. This post-orogenic transition between calc-alkaline to alkaline magmatism is an interesting phenomenon with similar examples in Uruguay (Oyhantcabal et al. 2007), Algeria (Coulon et al. 2002) and the Mediterranean (Maury et al. 2000) explained by slab tear. The emplacement of post-orogenic (~636 Ma) magmatism in the southern Nabitah Belt is considered to reflect the termination of east-west accretion (Robinson et al., 2014) and according to Flowerdew et al. (2013), a tear in the subducting slab evoked by extension. Adding to the Flowerdew et al. (2013) interpretation, the most favoured mechanism for LREE enrichment of CM A-types following slab tear is melting of the lower crust in the mantle wedge and perhaps the development of a depleted lower crustal MASH zone (Smithies et al. 2010). This long lived (~636 – 608 Ma; dated Al Hafoor and Kawr Suites) MASH zone would then homogenise and allow magma plumes to tap off and fractionate towards the surface. This large window of Nabitah Belt A-type magmatism (~30 Ma) is emphasised when

compared to the <5 Ma transition of the contaminated A-type Admar Suite (~600 Ma) and the appearance of the enriched A-type Al Bad Suite (~597 Ma) in the Midyan-Hijaz area of the Arabian Shield. It is therefore proposed that a lower crustal MASH zone mechanism beneath the Nabitah Suture can not only account for the large A-type window, but also the contaminated N-MORB and/or arc-tholeiite like geochemistry of the mafic parents which fractionate to both magnesian/VAG I-A-type and ferroan/WPG A-type granitoids. This process is in agreement with Kerr and Fryer (1993) and Han et al. (1997) who propose A-type generation from N-MORB systems in Canada and China respectively.

(**insert Figure 11**).

According to Robinson et al. (2014), the emplacement of EM suites at ~ 600 Ma is suggestive of another tectonic process. The ~ 585 Ma Abanat suite (AAPG) and closely associated ~ 607 Ma Idah Suite (POPG) are A-type alkali-granites emplaced into the northern end of the Nabitah Belt and are great examples to compare the transition from CM - VAG to EM - WPG tectonic environments. Alongside NHSG suites in the southern Nabitah Belt, the Idah Suite in the northern Nabitah Belt is also interpreted to result from a contaminated MORB/arc-tholeiite mantle in a lower crustal MASH zone (mantle wedge) in the final stages of the Ha'il and Afif - Ad Dawadimi terrane accretion. However, the Abanat Suite intrudes the Idah Suite and is HREE enriched, which according to Johnson (2006) marks a change in Arabian Shield mantle geochemistry. Both are classified as ferroan A-types, but are generated by differing mantle sources (**Figure 9**). It is suggested that the generation of the 607 Ma Idah Suite is associated with lower crustal melting following accretion. The Ha'il-

northern Afif lithosphere became so dense that it delaminated (Avigad and Gvirtzman, 2009) and allowed enriched mantle upwelling (limited crust-mantle interaction) marked by the appearance of the ~585 Ma Abanat Suite in the same location. One might argue that the change in mantle chemistry between the Idah and Abanat Suites may result from slab tear or intense fractionation rather than lithospheric delamination. It is suggested this is invalid because the AAPG suites are geochemically and isotopically distinct (**Figure 10**) from the similar mineralogy of NHSG and POPG intrusions that exhibit fractionation in subduction settings.

Although data presented in this study cannot conclusively point to delamination for limited-crust mantle A-type granitoids, it is the preferred mechanism to account the change to enriched mantle at <600 Ma. In addition to the Abanat and Idah Suites, the Midyan Terrane (north-western Shield) exhibits a similar post-orogenic to anorogenic petrogenetic transition, which is supported by the changing post-orogenic-anorogenic mantle described in Azer and Farahat (2011), Eyal et al. (2010) and Harris et al. (1986a). The ~600 Ma A-type Admar Suite (Hijaz) has a typical contaminated volcanic arc signature and <5 Ma later, the ~597 Ma A-type Al Bad Suite is produced (Midyan) with a HREE enriched geochemistry similar to the Al Hawiyah Suite (~591 Ma) in the southern Shield and Abanat Suite (~585 Ma) in the eastern Shield. As illustrated in **Figure 11**, these enriched A-types are clearly spatially intra-plate (also geochemically classified as WPG). By contrast, the contaminated, highly fractionated A-types such as the ~611 Ma Kawr Suite intrude major orogenic sutures (geochemically classified as VAG- and WPG) or in the case of the ~600 Ma Admar Suite, reside in the Hijaz volcanic arc intruding older (~700 Ma) synorogenic magmatism (both geochemically classified as VAG). This spatial observation is

supported by geochemical differences and indicates that a change in petrogenetic mechanism must occur. It should be noted that the ~525 Ma A-type syenite (mr) in the Hijaz terrane is not considered a product of lithospheric delamination, but as discussed in Robinson et al. (2014), rather a product of localised Najd Fault extension. The EM nature of this isolated syenite would then suggest that the Najd Fault possibly taps enriched mantle similar in geochemistry to suites derived from lithospheric delamination. According to Avigad and Gvirtzman (2009), the mantle associated with lithospheric delamination is asthenospheric enriched mantle. The REE signatures of this syenite are distinctly absent of Rb, K, U enrichment and negative Nb anomalies and according to Robinson (2014) are more OIB-like. It is therefore suggested that the mantle source associated with AAPG suites is OIB-like.

5.3. Regional tectonic implications for the Arabian-Nubian Shield

Arabian granitoid isotopic signatures and MORB like geochemistry would appear to complement Stoeser and Frost (2006), Be'eri-Shlevin et al. (2010) and Be'eri-Shlevin et al. (2012) who propose a depleted mantle beneath the ANS influenced by pre-Neoproterozoic crust. However, an enriched source with limited crust-mantle interaction is also apparent amongst <600 Ma A-types. This supports Stein and Goldstein (1996) for an enriched mantle beneath the ANS. However, data from this study indicate that this change in mantle occurs only at ~600 Ma, which coincides with a change in tectonic process discussed by Robinson et al. (2014). Although these data cannot rule out ~600 Ma mantle enrichment created by upwelling plumes that can be geochemically traced back to ~1000 Ma (Stein and Goldstein, 1996), this paper does not substantiate this mechanism for ANS magmatism between

~845 and 600 Ma. Instead, this study suggests subduction and accretion between ~845 and 600 Ma involving contaminated MORB-/arc-tholeiite-like magmatism. This is then followed by lithospheric delamination associated with upwelling enriched mantle (OIB-like) confined to within-plate and back-arc settings, which is in agreement with Avigad and Gvirtzman (2009) and the ~ 600 Ma final consolidation of the ANS (Collins and Pisarevsky, 2005).

The accretion and extension cycles and switch between mantle types involved in the Arabian Shield also appears to be consistent in style across the ANS. Data from this study is plotted with I- and A-type data from other ANS countries (**Figure 12**) and three trends are produced: **1)** IA+Syn, POPG and NHSG form the Arabian CM trend, **2)** Jordan, Israel and some Arabian AAPG data form the second contaminated mantle trend (possibly the transition), and **3)** Egypt, Yemen and some Arabian AAPG data create the EM trend. These trends indicate that post-orogenic and anorogenic granitoids involve a decrease in crust-mantle interaction with increasing Nb, hence two mantle types. This process may reflect first subduction followed by lithospheric delamination and may also help to explain the transition from post-orogenic calc-alkaline to anorogenic alkaline magmatism documents in other ANS regions such as Sinai (Azer and Farahat, 2011; Eyal et al. 2010).

(**insert Figure 12**).

6. Conclusions

Geochronology and whole-rock geochemistry defines and distinguishes four discrete granite-dominated igneous suites: 1) ~ 845 – 700 Ma island arc and synorogenic granitoids (IA+Syn), 2) ~ 640 – 610 Ma granitoids from the Nabitah and Halaban Suture (NHSG), 3) ~ 610 – 600 Ma post-orogenic perthitic (hypersolvus) granitoids (POPG), and 4) <600 Ma anorogenic aegirine-bearing perthitic (hypersolvus) granitoids (AAPG). Major and trace element chemistry distinguish groups 1, 2 and 3 as I-S- and A-type granites with REE signatures typical of volcanic arc settings (Rb, Ba, K, U enrichment and negative Nb anomalies) and extensive fractionation from mafic parental magmas that produce both calc-alkaline – alkaline and VAG – WPG magmatism. By contrast, group 4 A-types are distinctly more enriched in HREE (e.g. Nb, Rb, Ga, Nd, Zr and Y) and are interpreted to be emplaced into within-plate back - arc settings.

Nd isotopic signatures, combined with the fractional crystallisation dominant behaviour of groups 1, 2 and 3 (~ 5 – 180 Ce/Yb ratios), revealed two distinct A-types are generated in the Arabian Shield. Groups 1 and 2 gabbros are MORB and arc-tholeiite-like and isotopically lie within the upper field of the Paleoproterozoic Khida terrane ($\varepsilon Nd + 1$), which may indicate a crustal component in the parental source i.e. crustal assimilation followed by fractionation. These are quite distinct from the unfractionated (~ 1 – 40 Ce/Yb ratios), more juvenile ($\varepsilon Nd + 5$) group 4 suites suggestive of limited crust-mantle interaction. Nb and Y are used to support a model for two Shield mantle sources supporting Harris et al. (1986a): contaminated mantle (CM), which includes groups 1, 2, and 3, and enriched mantle (EM) defined by group 4. The former exhibits linear style fractionation trends constrained by 1 – 40 ppm Nb and up to 1 – 200 ppm Y. This depleted CM is thought to be a long lived, lower

crustal MASH zone formed during subduction/accretion (possibly within the mantle wedge). By contrast, within-plate group 4 suites are characterised by > 40 – 80 ppm Nb and 30 – 70 ppm Y and combined with their isotope and REE geochemistry, suggests a new enriched mantle source (possibly OIB-like) that may reflect lithospheric delamination. Although the data and petrogenetic interpretations presented in this study can be suggested for the Midyan, Hijaz, northern and eastern Asir, Tathlith, Ha'il, Afif and Ad Dawadimi Terranes, they cannot be substantiated for the Ar Rayn Terrane or the majority of the Asir Terrane. It is suggested that these processes may be applicable to these two terranes, but further geochemical study would be required to valid these claims.

Acknowledgments

The Saudi Geological Survey, in particular Khalid Kadi and Mubarak M Nahdi, are thanked for providing research funding and gracious hospitality in Saudi Arabia during February 2010 field work. David Bruce and John Stanley from the University of Adelaide and Aoife McFadden from the Adelaide Microscopy are also thanked for help in obtaining whole-rock geochemistry and isotope data. Dr Peter Johnson is greatly appreciated for his contributions to the Arabian Shield data interpretation presented in this paper. This paper forms TRax Record #313.

Appendix A. Supplementary whole-rock major and trace element data

Appendix B. Supplementary whole-rock Nd-Sm and Sr isotope data

Appendix C. Supplementary analytical techniques

References

Abdel-Rahman, A-F.M. and Martin, R.F. (1990). The Mount Gharib A-type granite, Nubian Shield: Petrogenesis and role of metasomatism at the source. *Contributions to Mineralogy and Petrology* **104**, 173-183.

Avigad, D. and Gvirtzman, Z. (2009). Late Neoproterozoic rise and fall of the northern Arabian-Nubian Shield: The role of lithospheric mantle delamination and subsequent thermal subsidence. *Tectonophysics* **477**, 217-228.

Azer, M.K. and Farahat, E.S. (2011). Late Neoproterozoic volcano-sedimentary successions of Wadi Rufaiyil, southern Sinai, Egypt: A case of transition from late-to pos-collisional magmatism. *Journal of Asian Earth Sciences* **42**, 1187-1203.

Batchelor, R.A. and Bowden, P. (1985). Petrogenetic interpretation of granitoid rock series using multicationic parameters. *Chemical Geology* **48**, 43-55.

Be'eri-Shlevin, Y., Eyal, M., Eyal, Y., Whitehouse, M.J. and Litvinovsky, B. (2012). The Sa'al volcano-sedimentary complex (Sinai, Egypt): A latest Mesoproterozoic volcanic arc in the northern Arabian-Nubian Shield. *Geology* **40**, 403-406.

Be'eri-Shlevin, Y., Katzir, Y. Blichert-Toft, J., Kleinhanns, I.C. and Whitehouse, M.J. (2010). Nd-Sr-Hf-O isotope provinciality in the northern most Arabian-Nubian Shield: implications for crustal evolution. *Contributions to Mineralogy and Petrology* **160**, 181-201.

Bentor, Y.K. (1985). The crustal evolution of the Arabo-Nubian Massif with special reference to the Sinai Peninsular. *Precambrian Research* **28**, 1-74.

Black, R. and Liegeois, J-P. (1993). Cratons, mobile belts, alkaline rocks and continental lithospheric mantle: the Pan-African testimony. *Journal of the Geological Society* **150**, 89-98.

Bonin, B (2004). Do coeval mafic and felsic magmas in post-collisional to within-plate regimes necessarily imply two contrasting, mantle and crustal sources? A review. *Lithos* **78**, 1-24.

Bonin, B. (2007). A-type granites and related rocks: Evolution of a concept, problems and prospects. *Lithos* **97**, 1-29.

Brown, G.C., Thorpe, R.S. and Webb, P.C. (1984). The geochemical characteristics of granitoids in contrasting arcs and comments on magma sources. *Journal of the Geological Society* **141**, 413-426.

Coleman, R.G., DeBari, S. and Peterman, Z. (1992). A-type granite and the Red Sea opening. *Tectonophysics* **204**, 27-40.

Collins, A.S. and Pisarevsky, S.A. (2005). Amalgamating Eastern Gondwana: the evolution of the Circum-Indian Orogens. *Earth Science Reviews* **71**, 229-270.

Coulon, C., Megartsi, M., Fourcade, S. Maury, R.C., Bellon, H., Loumi-Hacini, A., Cotten, J., Coutelle, A. and Hermitte, D. (2002). Post-collisional transition from calc-alkaline to alkaline volcanism during the Neogene in Oranie (Algeria): magmatic expression of slab breakoff. *Lithos* **62**, 87-110.

Cox, G.M., Lewis, C.J., Collins, A.S., Halverson, G.P., Jourdan, F., Foden, J., Nettle, D. and Kattan, F. (2012). Ediacaran terrane accretion within the Arabian-Nubian Shield. *Gondwana Research* **21**, 341-352.

De la Roche, H., Leterrier, J., Grandclaude, P. and Marchal, M. (1980). A classification of volcanic and plutonic rocks using R1-R2-diagram and major element analyses-its relationships with current nomenclature. *Chemical Geology* **29**, 183-210.

Doebrich. J.L., Al-Jehani, A.M., Siddiqui, A.A., Hayes, T.S., Wooden, J.L. and Johnson, P.R. (2007). Geology and metallogeny of the Ar Rayn terrane, eastern Arabian shield: evolution of a Neoproterozoic continental-margin arc during assembly of Gondwana within the East African Orogen. *Precambrian Research* **158**, 17-50.

Eby, N.G. (1990). The A-type granitoids: A review of their occurrence and chemical characteristics and speculations on their petrogenesis. *Lithos* 26, 115-134.

El-Bialy, M.Z. and Streck, M.J. (2009). Late Neoproterozoic alkaline magmatism in the Arabian-Nubian Shield: the postcollisional A-type granite of Sahara-Umm Adawi pluton, Sinai, Egypt. *Arabian Journal of Geosciences* **2**, 151-174.

El-Gharbawy, R.I. (2011). Petrogenesis of granitic rocks of the Jabal Sabir area, South Taiz City, Yemen Republic. *Chinese Journal of Geochemistry* **30**, 193-203.

El-Sayed, M.M., Mohamed, F.H., Furnes, H. and Kanisawa, S. (2002). *Chemie der Erde Geochemistry* **42**, 317-346.

Eyal, M., Litvinovsky, B., Jahn, B.M., Zanvilevich, A. and Katzir, Y. (2010). Origin and evolution of post-collisional magmatism: Coeval Neoproterozoic calc-alkaline and alkaline suites of the Sinai Peninsula. *Chemical Geology* **269**, 153-179.

Flowerdew, M.J., Whitehouse, M.J. and Stoeser, D.B. (2013). The Nabitah fault zone, Saudi Arabia: A Pan-African suture separating juvenile oceanic arcs. *Precambrian Research* **239**, 95-105.

Frost, B.R., Barnes, C.G., Collins, W.J., Arculus, R.J., Ellis, D.J. and Frost, C.D. (2001). A Geochemical Classification for Granitic Rocks. *Journal of Petrology* **42**, 2033-2048.

Frost, C.D. and Frost, B.R. (2011). On ferroan (A-type) granitoids: their compositional variability and modes of origin. *Journal of Petrology* **52**, 39-53.

Gass, I.G., Ries, A.C., Shackleton, R.M. and Smewing, J.D. (1990). Tectonics, geochronology and geochemistry of the Precambrian rocks of Oman. *Geological Society, London, Special Publications* **49**, 585-599.

Goldstein, S.L., O'Nions, R.K. and Hamilton, P.J. (1984). A Sm-Nd isotopic study of atmospheric dusts and particulates from major river systems. *Earth and Planetary Science Letters* **70**, 221-236.

Goodge, J.W. and Vervoort, J.D. (2006). Origin of Mesoproterozoic A-type granites in Laurentia: Hf isotope evidence. *Earth and Planetary Science Letters* **243**, 711-731.

Han, B-f., Wang, S-g., Jahn, B-m., Hong, D-w., Kagami, H. and Sun, Y-l. (1997). Depleted-mantle source for the Ulungur River A-type granites from North Xinjiang, China: geochemistry and Nd-Sr isotopic evidence, and implications for Phanerozoic crustal growth. *Chemical Geology* **138**, 135-159.

Hargrove, U.S., Stern, R.J., Kimura, J.-I., Manton, W.I. and Johnson, P.R. (2006). How juvenile is the Arabian-Nubian Shield? Evidence from Nd isotopes and pre-Neoproterozoic inherited zircon in the Bi'r Umq suture zone, Saudi Arabia. *Earth and Planetary Science Letters* **252**, 308-326.

Harris, N.B.W., Duyverman, H.J. and Almond, D.C. (1983). The trace element and isotope geochemistry of the Sabaloka Igneous Complex, Sudan. *Journal of the Geological Society, London* **140**, 245-256.

Harris, N. B. W., Marzuki, F. M. H. and Ali,S. (1986a). The Jabel Sayid complex, Arabian Shield: geochemical constraints on the origin of peralkaline and related granites. Journal of the Geological Society London, 143, 287-295.

Harris, N.B.W., Pearce, J.A. and Tindle, A.G. (1986b). Geochemical characteristics of collision-zone magmatism. *Geological Society, London, Special Publications* **19**, 67-81.

Jarrar, G., Stern, R.J., Saffarini, G. and Al-Zubi, H. (2003). Late-and post-orogenic Neoproterozoic intrusions of Jordan: implications for crustal growth in the northernmost segment of the East African Orogen. *Precambrian Research* **123**, 295-319.

Jarrar, G.H., Manton, W.I., Stern, R.J. and Zachmann, D. (2008). Later Neoproterozoic A-type granites in the northernmost Arabian-Nubian Shield formed by fractionation of basaltic melts. *Chemie der Erde Geochemistry* **68**, 295-312.

Jenner, F.E. and O'Neil, H. C. (2012). Analysis of 60 elements in 616 ocean floor basaltic glasses. *Geochemistry, Geophysics, Geosystems* **13**, 1-11.

Johnson, P.R (2006). Explanatory notes to the map of Proterozoic geology of western Saudi Arabia. *Technical Report, Saudi Geological Survey*, **SGS-TR-2006-4/1427H 2006 G.**

Johnson, P.R., Andersen, A., Collins, A.S., Fowler, A.R., Fritz, H., Ghebreab, W., Kusky, T. and Stern, R.J. (2011). Late Cryogenian-Ediacaran History of the Arabian-Nubian Shield: A review of depositional, plutonic, structural, and tectonic events in the closing stages of the northern East African Orogen. *Journal of African Earth Sciences* **10**, 1-179.

Katzir, Y., Eyal, M., Litvinovsky, B.A., Jahn, B.M., Zanvilevich, A.N., Valley, J.W., Beeri, Y., Pelly, I. and Shimshilashvili, E. (2007). Petrogenesis of A-type granites and origin of

vertical zoning in the Katharina pluton, Gebel Mussa (Mt. Moses) area, Sinai, Egypt. *Lithos* **95**, 208-228.

Kerr, A. and Fryer, B.J. (1993). Nd isotope evidence for crust-mantle interaction in the generation of A-type granitoid suites in Labrador, Canada. *Chemical Geology* **104**, 39-60.

Klemenic, P.M. and Poole, S. (1988). The geology and geochemistry of Upper Proterozoic granitoids from the Red Sea Hills, Sudan. *Journal of the Geological Society, London* **145**, 635-643.

Maury, R.C., Fourcade, S., Coulon, C., El Azzouzi, M., Bellon, H., Coutelle, A., Ouabadi, A., Semroud, B., Megartsi, M., Cotten, J, Belanteur, O., Louni-Hacini, A., Pique, A., Capdevila, R., Hernandez, J. and Rehault, J-P. (2000). Post-collisional Neogene magmatism of the Mediterranean Maghreb margin: a consequence of slab breakoff. *Earth and Planetary Sciences* **331**, 159-173.

Meschede, M. (1986). A method of discriminating between different types of mid-ocean ridge basalts and continental tholeiites with the Nb-Zr-Y diagram. *Chemical Geology* **56**, 207-218.

Moghazi, A.M. (2002). Petrology and geochemistry of Pan-African granitoids, Kab Amiri area, Egypt - implications for tectonomagmatic stages in the Nubian Shield evolution. *Mineralogy and Petrology* **75**, 41-67.

Moufti, A.M.B., Ali, K.A., Whitehouse, M.J., 2013. Geochemitsry and petrogenesis of the Ediacaran post-collisional Jabal Al-Hassir ring complex, Southern Arabian Shield, Saudi Arabia. Chemie der Erde 73, 451-467.

Mushkin, A., Navon, O., Halicz, L., Hartmann, G. and Stein, M. (2003). The petrogenesis of A-type magma from the Amram Massif, Southern Israel. *Journal of Petrology* **44**, 815-832.

Nettle, D., Halverson, G.P., Cox, G.M., Collins, A.S., Schmitz, M., Gehling, J., Johnson, P.R., Kadi, K. (2014). A Middle-Late Ediacaran Volcano-sedimentary Record from the Eastern Arabian-Nubian Shield. *Terra Nova* **26**, 120-129.

Oyhantcabal, P., Siegesmund, S., Wemmer, K., Frei, R. and Layer, P. (2007). Post-collisional transition from calc-alkaline to alkaline magmatism during transcurrent deformation in the southernmost Dom Feliciano Belt (Braziliano-Pan-African, Uruguay). *Lithos* **98**, 141-159.

Pearce, J.A., Harris, N.B.W. and Tindle, A.G. (1984a). Trace element discrimination diagrams for the tectonic interpretation of granitic rocks. *Journal of Petrology* **25**, 956-983.

Pearce, J.A., Lippard, S.J. and Roberts, S. (1984b). Characterisation and tectonic significance of supra-subduction zone ophiolites. *Geological Society of London, Special Publications* **16**, 77-94.

Robinson, F.A. (2014). Geochronological and geochemical constraints on the lithospheric evolution of the Arabian Shield, Saudi Arabia: Understanding plutonic rock petrogenesis in an accretionary orogen. *Doctoral dissertation, The University of Adelaide, South Australia.*

Robinson, F.A., Foden, J.D., Collins, A.S. and Payne, J.L. (2014). Arabian Shield magmatic cycles and their relationship with Gondwana assembly: Insights from zircon U-Pb and Hf isotopes. *Earth and Planetary Science Letters* **408**, 207-225.

Smithies, R.H., Howard, H.M., Evins, P.M., Kirkland, C.L., Kelsey, D.E., Hand, M., Wingate, M.T.D., Collins, A.S. and Belousova, E. (2011). High-temperature granite magmatism, crust-mantle interaction and the Mesoproterozoic intercontinental evolution of the Musgrave Province, Central Australia. *Journal of Petrology* **52**, 931-958.

Sossi, P.A., Foden, J.D. and Halverson, G.P. (2012). Redox-controlled iron isotope fractionation during magmatic differentiation: an example from the Red Hill Intrusion, S. Tasmania. *Contributions to Mineralogy and Petrology* **164**, 757-772.

Stein, M. and Goldstein, S.L. (1996). From plume head to continental lithosphere in the Arabian-Nubian shield. *Nature* **382**, 773-778.

Stern, R.J., Ali, K.A., Liegeois, J.P., Johnson, P.R., Kozdroj, W. and Kattan, F.H. (2010). Distribution and significance of pre-Neoproterozoic zircons in juvenile Neoproterozoic igneous rocks of the Arabian-Nubian Shield. American Journal of Science 310, 791-811.

Stoeser, D.B. and Camp, V.E. (1985). Pan African microplate accretion of the Arabian Shield. *Geological Society of American Bulletin* **96**, 817-826.

Stoeser, D.B. and Frost, C.D. (2006). Nd, Pb, Sr and O isotopic characterisation of Saudi Arabian Shield terranes. *Chemical Geology* **226**, 163-188.

Sun, S.-S. and McDonough, W.F. (1989). Chemical and isotopic systematics of oceanic basalts: implications for mantle composition and processes. G*eological Society of London, Special Publications* **42**, 313-345.

Tanaka, T., Togahi, S., Kamioka, H., Amakawa, H., Kagami, H., Hamamoto, T., Yuhara, M., Orihashi, Y., Yoneda, S., Shimizu, H., Kunimaru, T., Takahashi, K., Yanagi, T., Nakano, T., Fujimaki, H., Shinjo, R., Asahara, Y., Tanimizu, M. and Dragusanu, C. (2000). JNdi-1: a neodymium isotopic reference in consistency with LaJolla neodymium. *Chemical Geology* **168**, 279-281.

Turner, S. and Foden, J. (1996). Magma mingling in late-Delamerian A-type granites at Mannum, South Australia. *Mineralogy and Petrology* **56**, 147 – 169.

Turner, S. Foden, J. and Morrison, R.S. (1992). Derivation of some A-type magmas by fractionation of basaltic magma: An example from the Padthaway Ridge, South Australia. *Lithos* **28**, 151-179.

Whalen, J.B., Currie, K.L. and Chappell, B.W. (1987). A-type granites: geochemical characteristics, discrimination and petrogenesis. *Contributions to Mineralogy and Petrology* **95**, 407-419.

Figure 1: A geological map of the Arabian Shield taken from Robinson et al. (2014) highlighting 20 sampled suites (blue dotes) and their respective tectonic timing. Sample location numbers corresponding to suite names are presented in **Table 1**. Symbol a = Yanbu Suture (~715 Ma collision of Midyan-Hijaz Terranes), b = B'ir Umq Suture (~780−680 Ma collision of Hijaz-Asir Terranes), c = Nabitah Suture (~680−640 Ma collision of Hijaz-Afif Terranes), d = Nabitah Suture (~680 − 640 Ma collision of Asir-Afif Terranes), and e = Halaban Suture (~700 − 600 Ma collision of Afif-Ad Dawadimi+Ar Ryan Terranes).

Figure 2: Petrographic images from a selection of the granitoids representing the four tectonic groups sampled across the Arabian Shield. **A**) The island arc (~845 Ma) Makkah Suite Granodiorite-tonalite is taken from the Asir terrane (western Shield) and exhibits extensive mingling with gabbroic dykes. **B)** The synorogenic (~705 Ma) Jar-Salajah Complex is a typical granodiorite suite found confined to the Yanbu Suture area of the Hijaz Terrane (western Shield). **C)** The post-orogenic Kawr Suite (~611 Ma) was collected in the Nabitah Belt (west-east Shield collision) and is associated with extensive gabbroic, dioritic, granitic and aegirine-bearing alkali-granite mingling (two photos). **D)** The Abanat Suite (~585 Ma) is a classic aegirine-bearing alkali-granite taken from the Ha'il terrane (northern Shield) and contains no obvious mingling phases. Mineral abbreviations are displayed in **Table 1**.

Figure 3: Harker diagrams for sampled Arabian Shield granitoids divided into four tectonic age groups. Arabian suite abbreviations are presented in **Table 1** and the black square is the average MORB value (2SD error bars attached) taken from Jenner and O'Neil (2012). The background crosses are I- and A-type granite data from the ANS (references in **Table 1**).

Figure 4: Granitic classification schemes from Whalen et al. (1987), Frost et al. (2001) and Pearce et al. (1984a) applied to the four Arabian Shield granitoid groups. Note mafic intrusive samples (< 60% SiO_2) from kw and ao suites are also plotted to highlight the composition range within these suites, but are not classified in these schemes.

Figure 5: Primitive mantle normalised REE patterns of sampled Saudi Arabian whole-rock samples. The grey field is the tectonic group composition range and the solid and dashed black lines are representative granite and gabbroic samples respectively. The red line is the average MORB composition taken from Jenner and O'Neil (2012). It should be mentioned that the large compositional range displayed in the post-tectonic (~640-600 Ma) field is attributed to the Kawr Suite. This suite contains cumulate gabbros with REE patterns ~100 times less than granitic end-members. Similarly, within the anorogenic (<600 Ma) field, the lowest values (below rt185) correlate with the garnet-bearing Malik Granite (leucogranite). Samples are normalised to primitive mantle values from Sun and McDonough (1989).

Figure 6: Mafic intrusive classification schemes by Pearce et al., (1984) and Meschede (1986) applied to gabbroic end-members sampled in the Arabian Shield. It should be noted that the low Y samples from plot A are not plotted in B because they contain no detectable Nb values. The symbols in plot B are as follows: D = N-type MORB; C = within-plate tholeiite; B = P-type MORB and AI = within-plate alkali-basalts.

Figure 7: **Top)** Age vs. εNd (t) plot for all sampled Arabian granitoids, associated gabbros and surrounding volcanics. The terrane fields are taken from Stoeser and Frost (2006). It should be noted that the Paleoproterozoic Khida Terrane field here is the upper limit whilst according to Hargrove et al. (2006), the mean εNd field is ~ -5 to -10. **Bottom)** εNd (t) vs. εHf (t) plot highlighting the decreasing juvenility of sampled Arabian granitoids The juvenile crust array (dashed line) is taken from Be'eri-Shlevin et al. (2010). The εHf (t) data are the average zircon values for each suite taken from Robinson et al. (2014).

Figure 8: A time space plot modified from Robinson et al. (2014) highlighting the spatial relationship and granitic classification of the four tectonic groups sampled in the Arabian Shield. Symbols are as follows: dashes = gabbro, squares = I-type granite, triangles = S-type granite, circles = hypersolvus A-type granite, hexagon = hypersolvus aegirine-bearing A-type granite. Dashes inside squares and crosses inside circles/hexagons represent suites with gabbroic and gabbroic/dioritic/monzonitic samples respectively.

Figure 9: A mantle classification scheme for the Arabian Shield granitoids described as enriched mantle (EM) and contaminated mantle (CM). This figure distinguishes the trends associated with IA+Syn, NHSG and POPG from within-plate AAPG, hence differing mantle sources. Note that the ku suite (NHSG) is not illustrated here because it contains ~200 ppm Y and ~30 ppm Nb. The black square is the average MORB value (2SD error bars attached) taken from Jenner and O'Neil (2012). The within-plate granite field references are presented in **Table 1**.

Figure 10: A) Y/Nb vs. Ce/Yb illustrating the fractional crystallisation trend (non-calculated) involved in producing NHSG (CM) granitoids and the isolation of AAPG (EM) granitoids suggestive of a differing mantle source. **B)** and **C**) SiO2 vs. Nb and Mg# vs. Nb plots are used as an index of fractionation and indicate A-type granites contain two fields, which possibly indicates an enriched source with a reduction in crustal involvement. **D**) Nd (t) vs. SiO_2 highlights the differing sources of NHSG and IA+Syn gabbros (CM) associated with the Paleoproterozoic Khida terrane (upper field taken from Stoeser and Frost, 2006; lower mean value taken from Hargrove et al. 2006) and limited-crust mantle of younger magmatism. The

granitic products are split into hypersolvus and aegirine-bearing hypersolvus groups. The black square is the average MORB value (2SD error bars attached) taken from Jenner and O'Neil (2012).

Figure 11: A summary map of the geochemical characteristics of Arabian granitoids using schemes from Pearce et al. (1984a), Frost et al. (2001) and Whalen et al. (1987). The wide range in A-type settings correlates with both subduction and within-plate/back-arc related environments, hence the potential for differing mantle sources. Note the blue ferroan alkali-granites correlate with the Idah Suite (classified as VAG), which are distinguished from the red ferroan alkali-granites of the younger Abanat suite (classified as WPG).

Figure 12: Arabian data from this study are plotted as yellow circles (IA+Syn, POPG and NHSG) and red squares (AAPG) and are applied to regional ANS I-A-type data (black circles and heavy dashed lines). These trends suggest two mantle sources occur throughout the ANS and produce A-types associated with contaminated mantle (CM) and those derived form a more enriched source (EM). Note that the ku suite (NHSG) is note illustrated here because it contains ~200 ppm Y and ~30 ppm Nb. The blue square is the average MORB value (2SD error bars attached) taken from Jenner and O'Neil (2012). The ANS data forming the CM trend are predominantly from Jordan and Israel, whilst the EM trend are from Egypt and Yemen (references in **Table 1**).

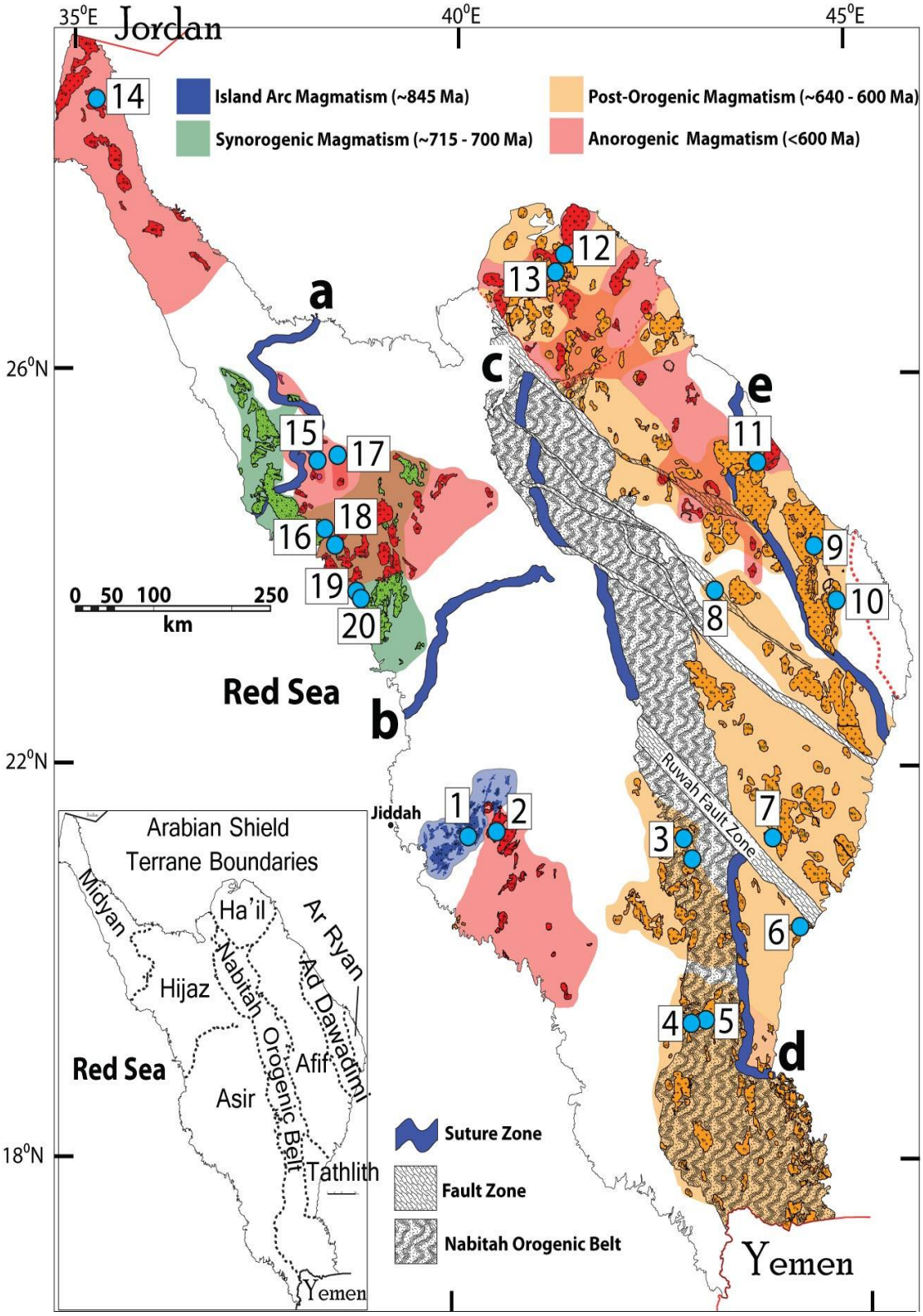

Figure 1.

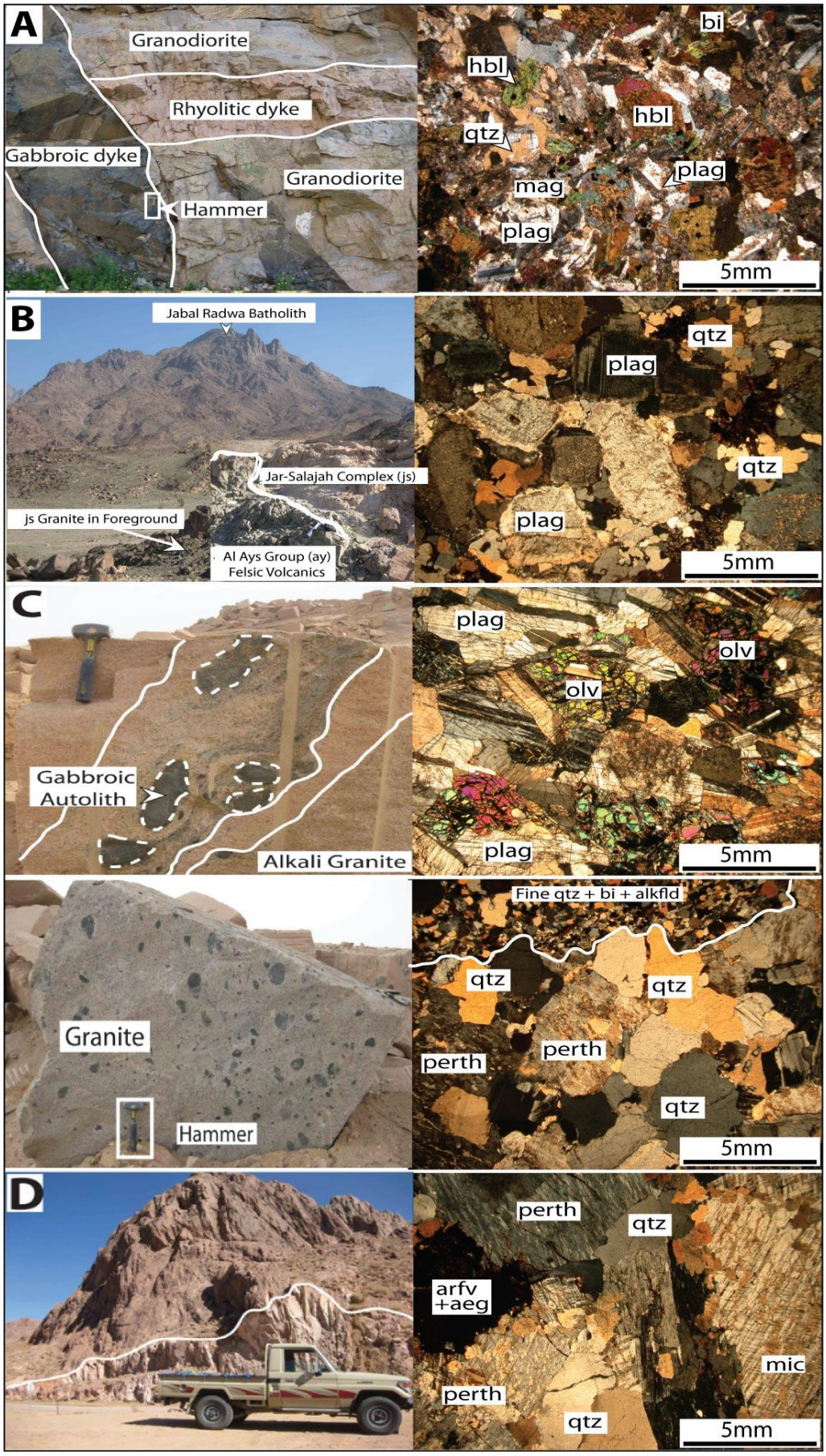

Figure 2.

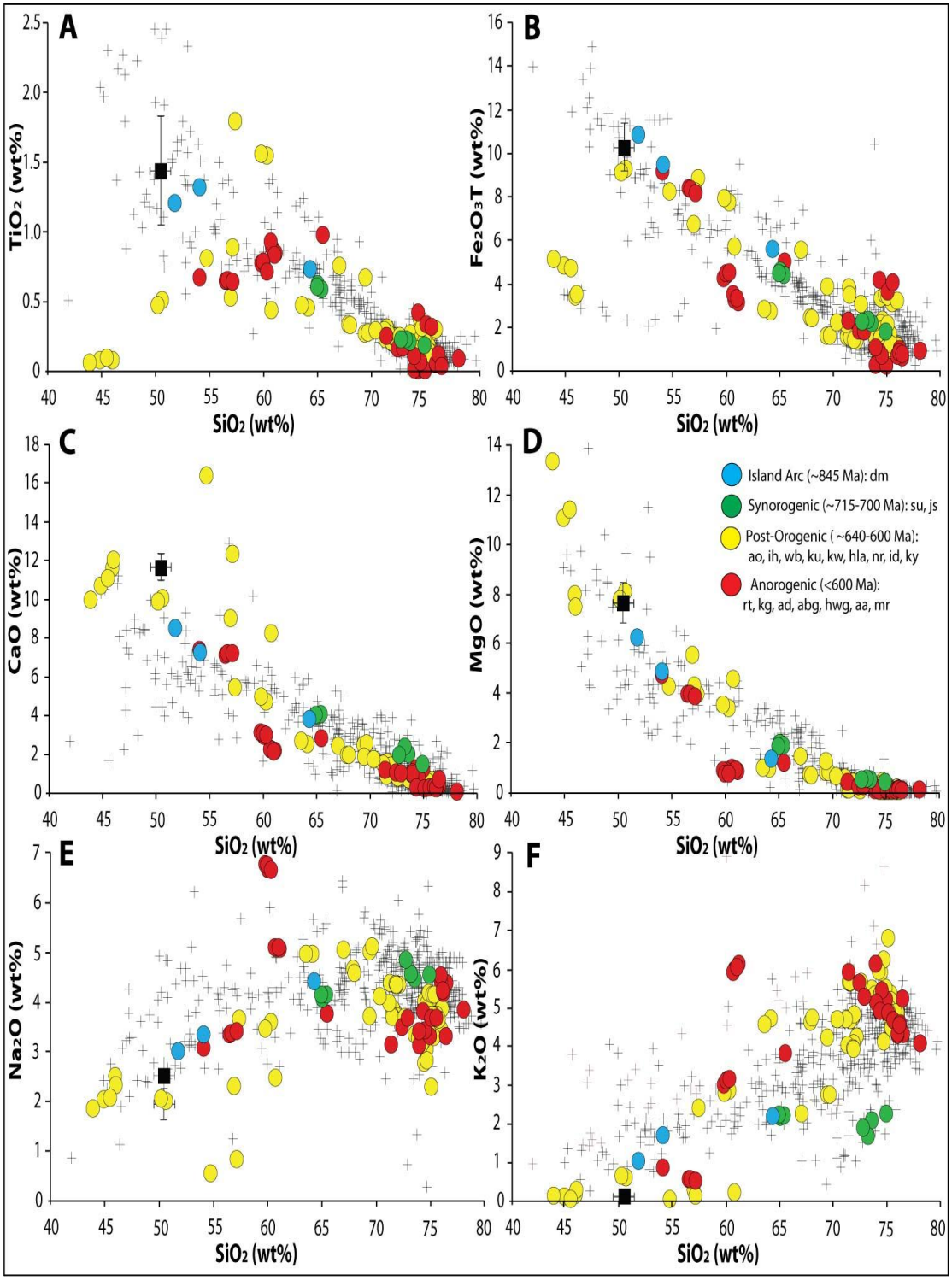

Figure 3.

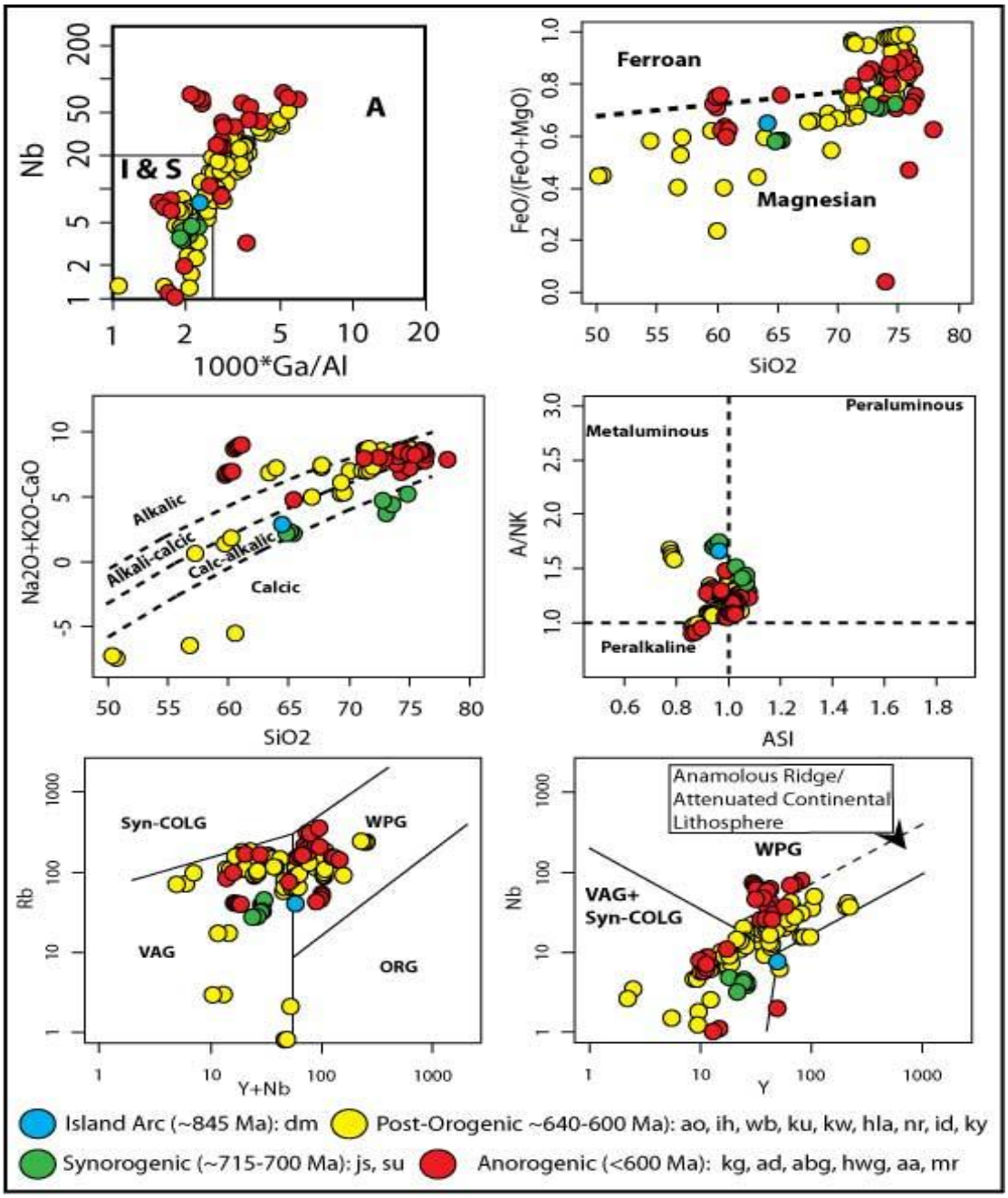

Figure 4.

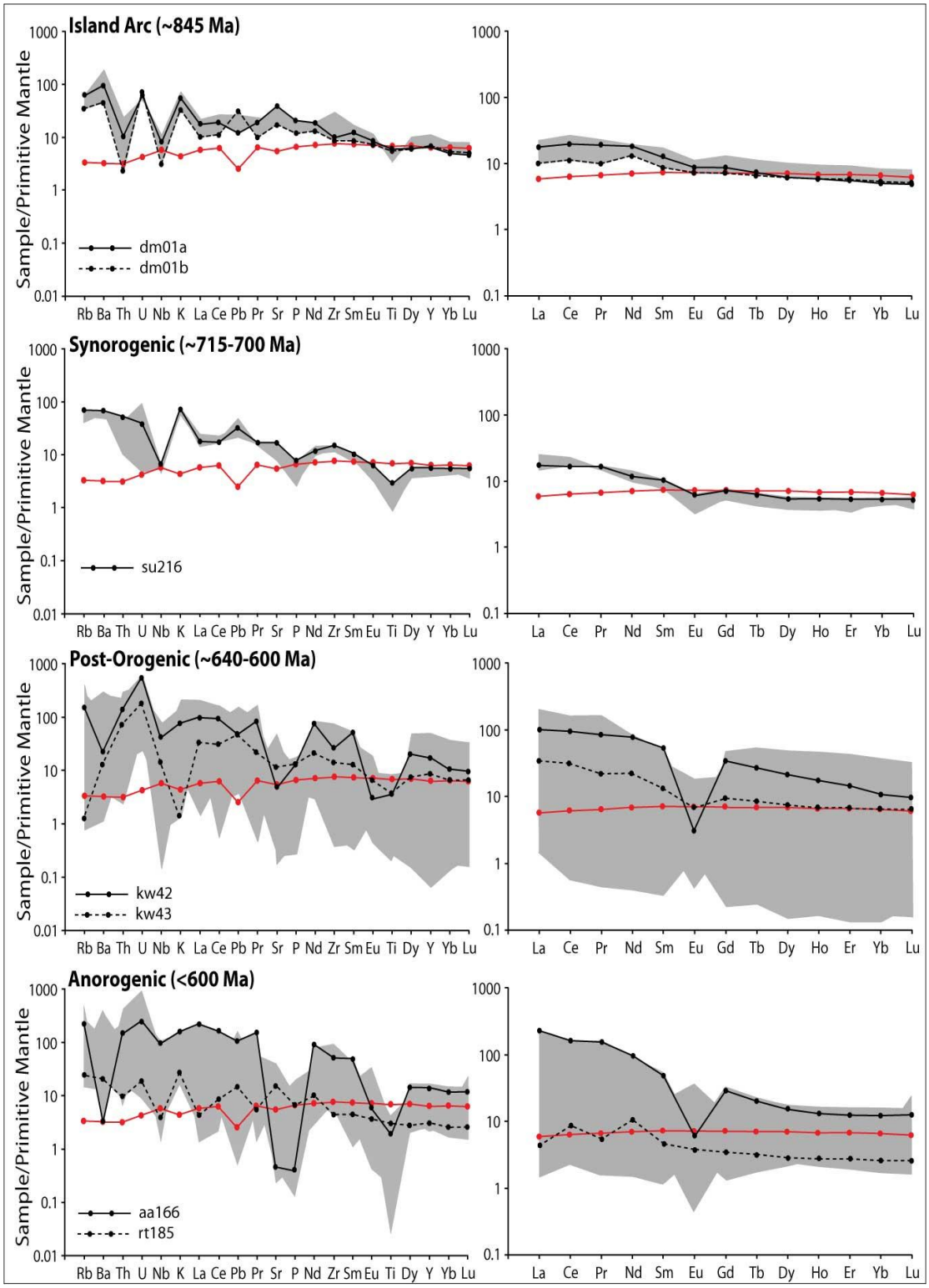

Figure 5.

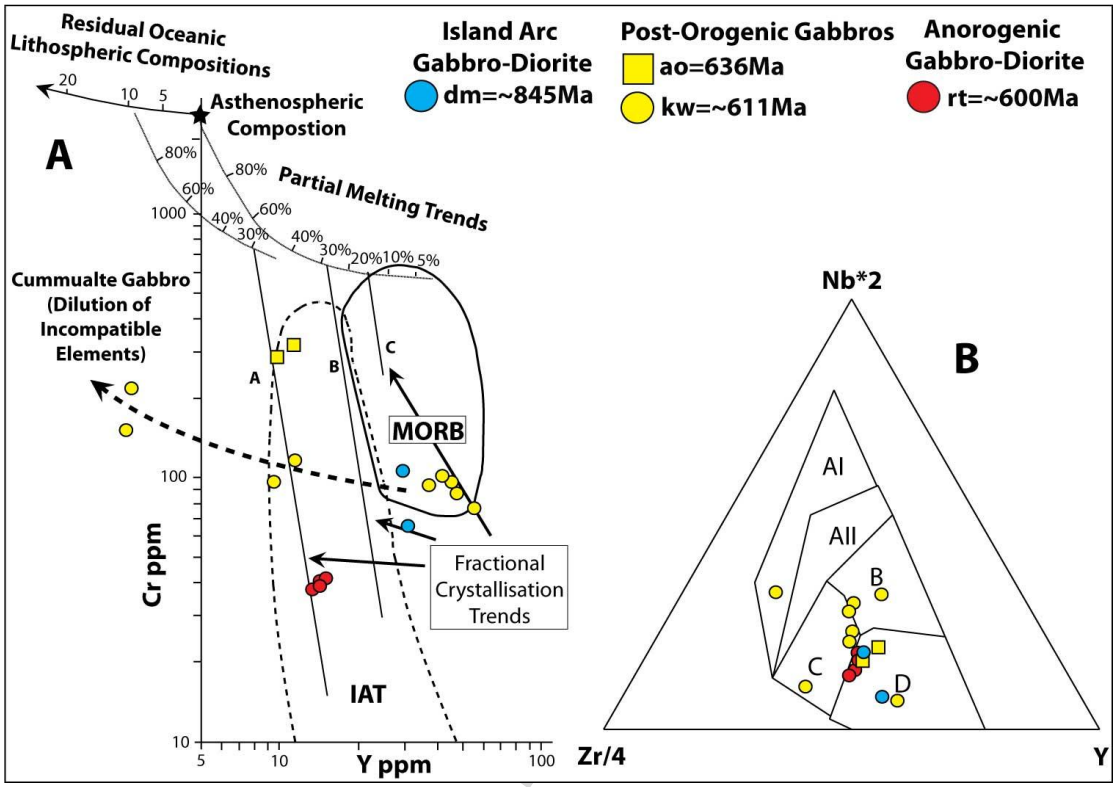

Figure 6.

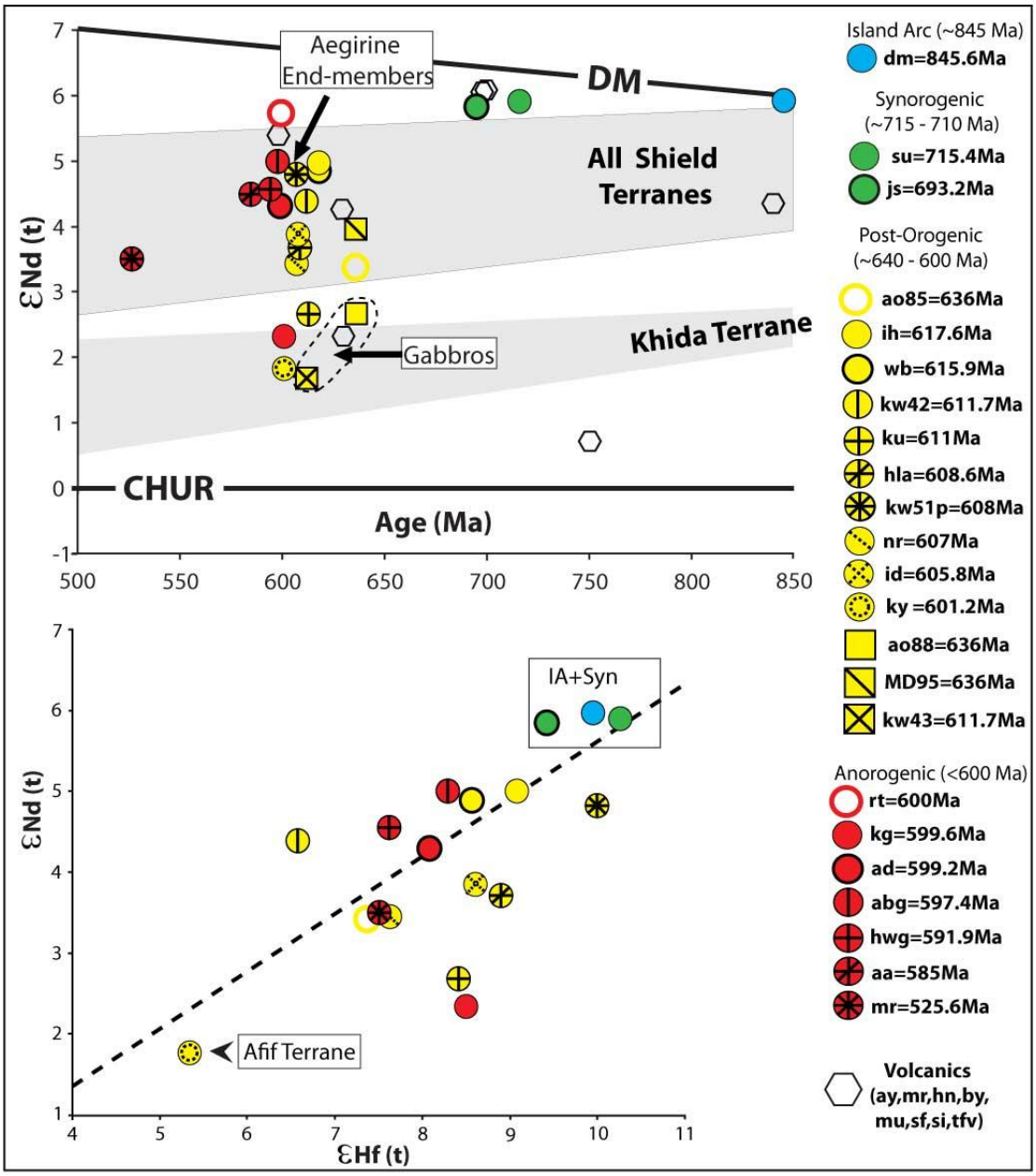

Figure 7.

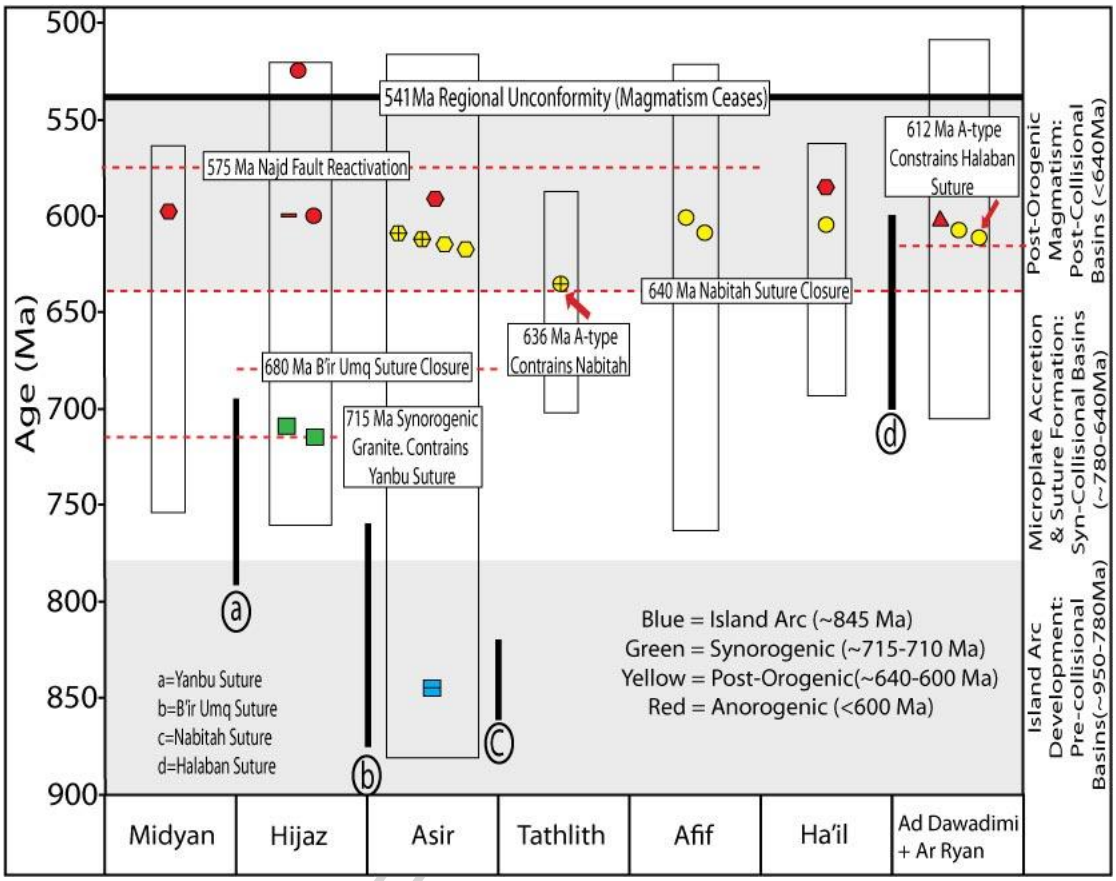

Figure 8:

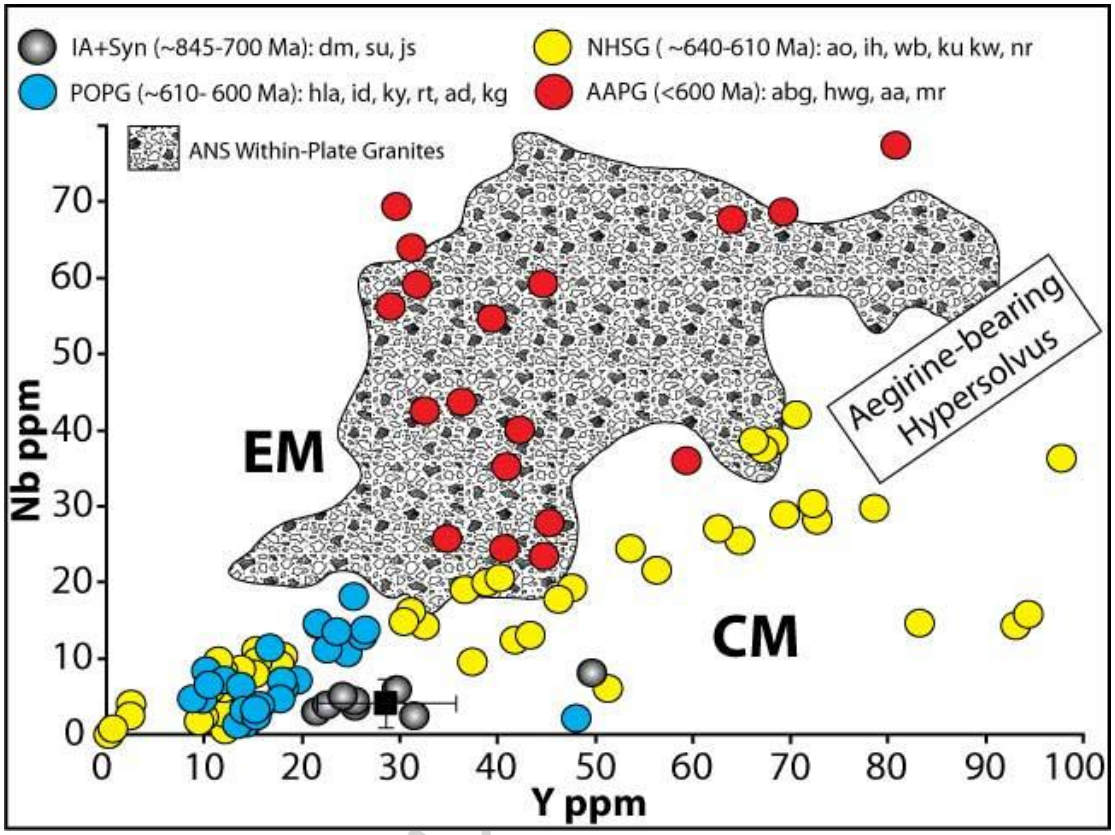

Figure 9.

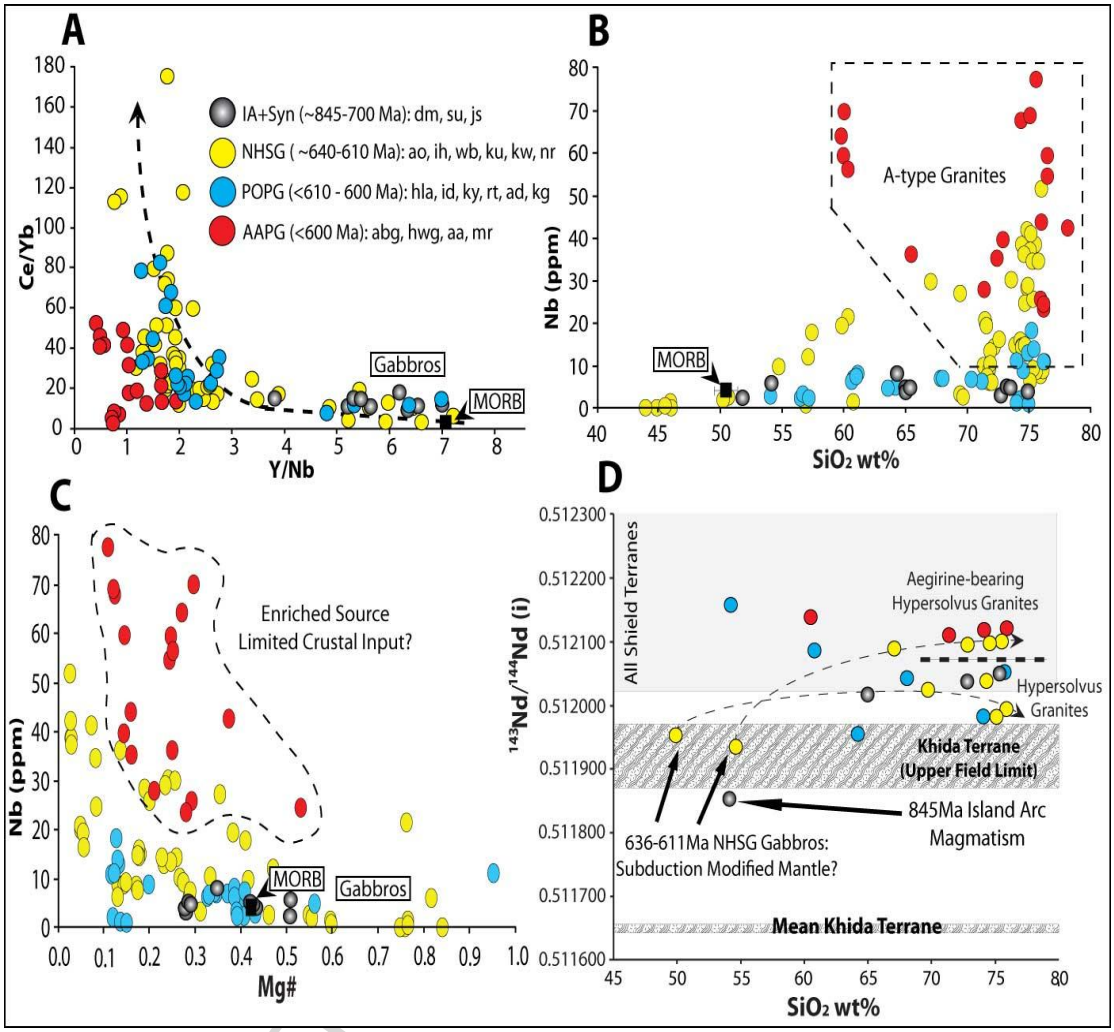

Figure 10.

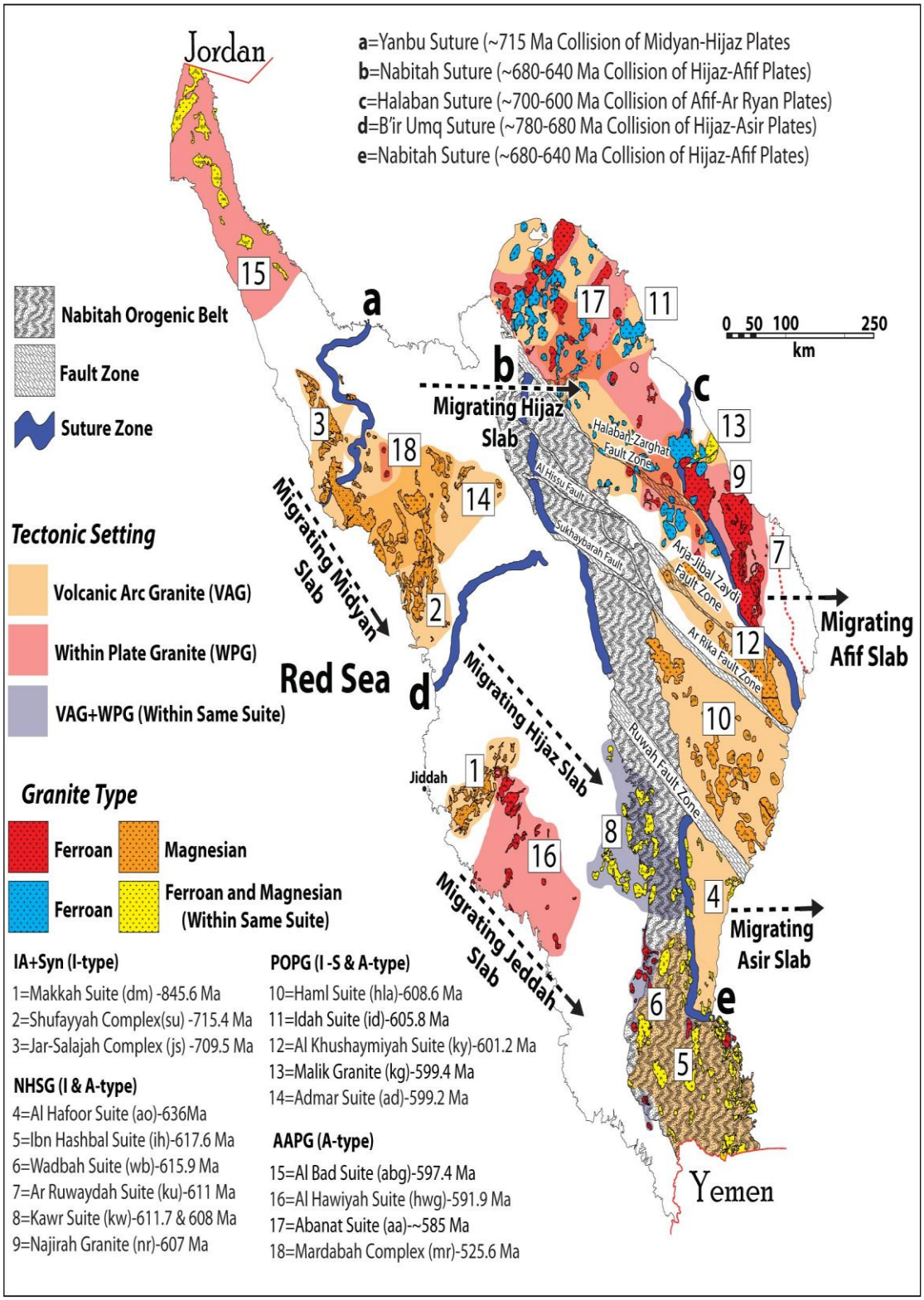

Figure 11.

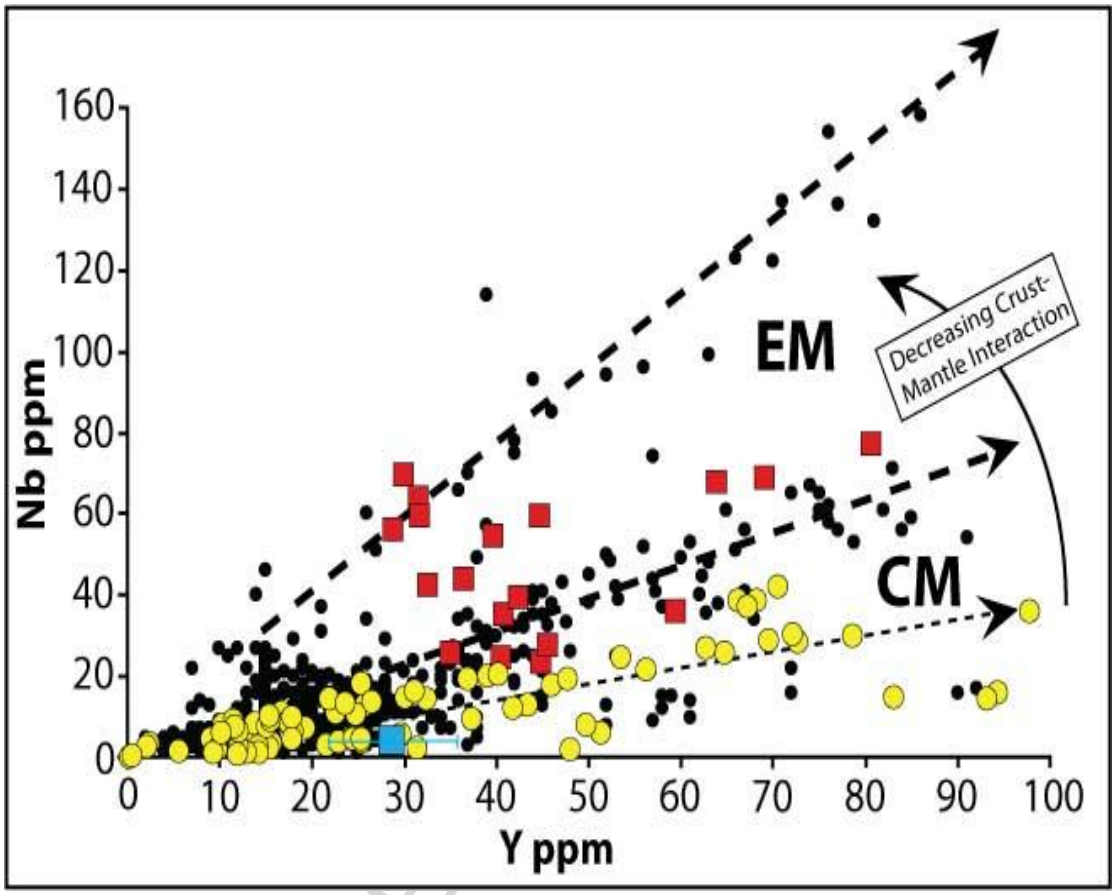

Figure 12.

Table 1: A petrographic and geochronology summary of the sampled plutons.

Shield Terrane	Geological Map Unit	No. Samples	Latitude	Longitude	Fig. 1. Location No.	Rock Type	Mineralogy	Hypersolvus (coarse perthite)	Na-rich Amphiboles & Pyroxenes	U-Pb age (Ma) Robinson et al. 2014	Tectonic Timing
Jiddah	Makkah Suiite (dm)	3	21° 21'36.45" N	40° 15'44.86" E	1	Gabbro-Tonalite	plag+hbl+bi+minor qtz+mag+ti			845.6	island arc
Hijaz	Shufayyah Complex (su)	3	23° 44'42.76" N	38° 46'50.11" E	20	Granodiorite/Tonalite	plag+qtz+hbl+bi. Accessory mag			715.4	synorogenic
Hijaz	Jar-Salajah Complex (js)	4	24° 24'37.62" N	38° 21'23.72" E	16	Granodiorite	qtz+plag+bi+alk-fld + minor mag and hbl			709.5	synorogenic
Hijaz	Subh Suite (sf)	4	23° 45'39.13" N	38° 45'09.74" E	19	Rhyolite	Rhyolite: alk-fld+qtz+plag (pheoncrysts). Groundmass=qtz+alk-fld			698.7	synorogenic
Tathlith	Al Hafoor Suite (ao)	8	20° 23'40.32" N	44° 18'05.19" E	6	Alkali-Granite	alk-fld+qtz+minor hbl+hast+bi. Accessory mag	✓		636	post-orogenic
Asir	Ibn Hasbal Suite (ih)	6	19° 29'13.91" N	42° 59'44.39" E	5	Alkali-Granite	mic+qtz+bi+minor plag+hbl+hast	✓	✓	617.6	post-orogenic
Asir	Wadbah Suite (wb)	4	19° 27'09.68' N	42° 49'58.70" E	4	Alkali-Granite	alk-fld+qtz+bi+minor hbl+mic+plag. Accessory mag+zirc	✓	✓	615.9	post-orogenic
Ad Dawadimi	Ar Ruwaydah Suite (ku)	4	24° 22'43.75" N	44° 21'40.56" E	9	Granite	alk-fld +qtz+plag+bi+minor mag+hast	✓		611	post-orogenic
			21° 20'04.76" N	42° 44'56.78" E		Gabbro	plag+olv+cpx+minor mag				
			21° 07'05.04' N	42° 53'16.43' E		Granite	qtz+alk-fld+plag+bi+minor mag+hast. Dioritic enclave=plag+hbl+cpx				
Asir	Kawr Suite (kw)	35	21° 20'10.17" N	42° 45'05.29" E	3	Alkali-Granite	alk-fld+qtz+aeg+minor bi+ti. Accessory mag+ap	✓	✓	611.7 & 608	post-orogenic
			20° 18'21.19" N	42° 41'39.41" E		Alkali-Granite	alk-fld+qtz+mic+minor bi. Accessory mag+ap. Granitic enclave+qtz+alk-fld+plag+minor hast+bi	✓	✓		
Afif	Haml Suite (hla)	4	21° 18'13.29" N	43° 51'21.78" E	7	Quartz- Monzonite	alk-fld+plag+minor qtz+hbl+mic+bi. Accessory mag+zirc+ap	✓		608.6	post-orogenic
Ad Dawadimi	Najirah Granite (nr)	4	23° 43'43.93" N	44° 41'21.06" E	10	Granite/Alkali-Granite	alk-fld+qtz+plag+bi+minor mag	✓		607	post-orogenic
Ha'il	Idah Suite (id)	5	27° 03'44.28" N	41° 17'58.70" E	13	Alkali-Granite	alk-fld+qtz+minor plag+hbl+bi+hast	✓		605.8	post-orogenic
Afif	Al Khushaymiyah Suite (ky)	5	23° 49'39.69" N	43° 11'42.07" E	8	Quartz-Monzonite	alk-fld+qtz+plag+hbl+minor mag+bi+mic+ti+hast	✓		601.2	post-orogenic
Hijaz	Rithmah Complex (rt)	4	25° 09'07.90" N	38° 11'20.41" E	15	Diorite/Gabbro	plag+cpx+hbl+minor olv+opx+mag			600*	anorogenic
Ad Dawadimi	Malik Granite (kg)	5	25° 07'56.42" N	43° 47'10.82" E	11	Leucogranite	qtz+alk-fld+minor plag+gt			599.4	anorogenic
Hijaz	Admar Suite (ad)	5	24° 17'53.09" N	38° 24'43.55" E	18	Syenite	alk-fld+bi+hbl+minor qtz+plag+mic+ti. Accessory mag+zirc+ap	✓		599.2	anorogenic
Midyan	Al Bad Granite Super Suite (abg)	6	28° 44'32.20" N	35° 20'12.32" E	14	Alkali-Granite	alk-fld+qtz+minor plag+bi. Accessory mag+zirc+ap+fl	✓	✓	597.4	anorogenic
Northern Asir	Al Hawiyah Suite (hwg)	5	21° 26'54.04" N	40° 27'16.45" E	2	Granite	alk-fld+qtz+bi+minor plag+hast+ti. Accessory mag	✓	✓	591.9	anorogenic
Ha'il	Abanat Suite (aa)	4	27° 18'43.63' N	41° 24'33.52" E	12	Alkali-Granite	alk-fld+qtz+minor plag+aeg+arfv	✓	✓	585*	anorogenic
Hijaz	Mardabah Complex (mr)	6	25° 11'29.42" N	38° 29'35.33" E	17	Syenite	alk-fld+bi+hbl+minor qtz+plag+olv. Accessory mag+zirc+ap	✓		525.6	anorogenic

References for ANS Geochemistry used in this study

I-type Granite: Egypt (Moghazi, 2002), Israel (Beyth et al. 1994), Oman (Gass et al. 1990) and Sudan (Klemenic and Poole, 1988).

Fractionated A-type Granite: Egypt (El-Sayed et al. 2002), Israel (Beyth et al. 1994) and Jordan (~250 data points from Jarrar et al. 2003 and Jarrar et al. 2008)

Within-plate A-type Granite: Egypt (Abdel-Rahman and Martin, 1990; El-Baily and Streck, 2009; Katzir et al. 2007), Israel (Mushkin et al. 2003), Sudan (Harris et al. 1983) and Yemen (Coleman et al. 1992; El-Gharbawy, 2011).

Note the coordinates, rock type and mineralogy displayed correlate with samples analysed for Nd-Sm and Sr isotopes, not the entire suite (all samples are described in Robinson (2014). U-Pb ages assigned an * are taken from Johnson (2006). Mineral abbreviations are as follows: aeg=aegirine, alk-fld=alkali-feldspar, ap=apatite, arfv=arfvedsonite, bi=biotite, cpx=clinopyroxene, fl=fluorite, gt=garnet, hast=hastingsite, hbl=hornblende, mag=magnetite, mic=microcline, opx=orthopyroxene, olv=olivine, plag=plagioclase, perth = perthite, qtz=quartz, ti=titanite and zirc=zircon.

Table 2: A summary of the XRF and solution ICPMS geochemistry for all 20 suites collected in the Arabian Shield.

Tectonic Timing	Island Arc (~845 Ma)		Synorogenic (~715 - 700 Ma)			Post-orogenic (~640 - 600 Ma)												Anorogenic (<600 Ma)						
	Makkah Suite		Shufayyah	Jar-Salajah	Subh Suite [sf]	Al Hafoor Suite		Ibn Hashbal Suite [ih]	Wadbah Suite [wb]	Ar Ruway-dah Suite [ku]	Kawr Suite				Haml Suite [hla]	Najirah Granite [nr]	Idah Suite [id]	Al Khushay-miyah Suite [ky]	Rithmah Complex [rt]	Mallik Granite [kg]	Admar Suite [ad]	Al Bad Suite [abg]	Al Hawiyah Suite [hwg]	Abanat Suite [aa]	Mardabah Complex [mr]
	[dm01a]	[dm01c]	Complex [su]	Complex [js]		[ao85]	[ao88]				[kw51p]	[kw42]	[kw43]	[kw14]											
SiO_2 (%)	54.13	64.34	64.98	72.78	75.35	76.00	50.23	74.71	72.65	75.18	75.60	67.05	54.77	44.90	68.04	74.44	75.43	64.18	54.11	74.01	60.82	76.23	71.43	74.38	60.35
TiO_2	1.32	0.73	0.60	0.23	0.12	0.09	0.47	0.31	0.25	0.07	0.13	0.76	0.81	0.08	0.33	0.15	0.10	0.45	0.67	0.11	0.89	0.12	0.25	0.42	0.72
Al_2O_3	15.47	15.74	15.96	14.53	12.98	12.36	17.09	12.39	12.98	12.99	12.93	14.03	15.60	22.42	15.96	13.25	12.95	17.72	17.53	13.92	18.37	12.49	14.00	10.76	18.06
Fe_2O_3	4.21	2.77	1.67	0.76	1.01	0.14	2.19	0.69	0.95	-0.04	0.04	0.82	1.58	0.95	0.92	0.11	0.21	1.19	2.18	1.06	1.49	0.55	0.54	3.39	1.97
FeO	4.72	2.54	2.52	1.35	0.36	0.91	6.22	1.08	1.91	1.12	0.75	4.27	5.97	3.50	1.36	1.23	0.93	1.38	6.27	0.01	1.57	0.39	1.59	0.72	2.31
Fe#	0.49	0.65	0.57	0.72	0.74	0.83	0.44	0.83	0.94	0.93	0.85	0.74	0.58	0.24	0.66	0.82	0.87	0.59	0.57	0.05	0.63	0.72	0.79	0.87	0.75
MnO	0.16	0.08	0.07	0.07	0.03	0.04	0.15	0.04	0.07	0.02	0.02	0.10	0.28	0.07	0.06	0.03	0.06	0.04	0.14	0.03	0.07	0.03	0.05	0.04	0.16
MgO	4.89	1.36	1.88	0.53	0.13	0.19	7.78	0.23	0.12	0.09	0.13	1.47	4.28	11.05	0.71	0.27	0.14	0.96	4.76	0.24	0.93	0.15	0.43	0.10	0.78
CaO	7.26	3.82	4.04	2.00	0.16	0.68	9.92	0.63	0.84	0.59	0.61	2.47	16.40	10.70	2.00	0.98	0.58	2.56	7.39	0.97	2.27	0.28	1.19	0.29	3.01
Na_2O	3.35	4.41	4.14	4.85	4.40	3.45	2.05	2.82	3.69	3.74	3.74	5.04	0.55	2.04	4.58	3.21	4.15	4.96	3.07	3.40	5.08	4.18	3.15	3.80	6.65
K_2O	1.69	2.18	2.23	1.89	4.06	4.89	0.65	6.24	5.65	4.89	5.00	2.26	0.04	0.10	4.75	5.38	4.48	4.71	0.86	5.12	5.99	4.59	5.92	4.91	3.14
P_2O_5	0.45	0.25	0.16	0.07	0.01	0.02	0.14	0.04	0.03	0.01	0.01	0.27	0.28	0.06	0.10	0.07	0.02	0.20	0.14	0.04	0.24	0.01	0.10	0.01	0.18
LOI %	1.48	0.63	1.22	0.47	0.63	0.62	2.24	0.28	0.37	0.29	0.26	0.36	0.00	3.99	0.41	0.39	0.36	0.39	2.62	0.56	0.31	0.40	0.61	0.48	1.12
Total %	99.67	99.15	99.76	99.68	99.27	99.50	99.83	99.61	99.73	99.68	99.30	99.38	101.12	100.29	99.38	99.65	99.52	98.91	100.45	99.49	98.21	99.47	99.43	99.39	98.70
Rb (ppm)	40.1	39.8	42.7	26.1	66.5	179.1	16.4	61.2	62.8	237.2	109.9	97.0	0.8	2.0	124.7	182.2	136.3	107.2	16.0	165.0	40.8	159.3	199.5	148.3	41.1
Ba	672.0	1268.0	469.0	403.0	689.0	159.0	228.0	178.0	318.0	21.0	171.0	151.0	91.0	48.0	1280.0	369.0	237.0	1982.0	149.0	337.0	2936.0	38.0	860.0	23.0	2185.0
Th	0.9	2.0	4.5	3.6	7.2	25.6	1.4	6.4	5.8	24.6	4.5	11.5	6.0	0.8	11.2	18.4	20.4	16.1	0.8	26.1	0.6	18.0	20.6	13.1	4.3
U	1.3	1.1	0.8	0.9	4.5	6.2	2.6	2.0	3.2	8.8	2.5	11.4	3.7	1.0	8.1	5.4	13.0	4.8	0.4	4.4	1.6	6.1	7.1	5.4	1.2
Nb	5.6	7.8	4.5	3.1	8.5	7.6	1.8	14.6	16.2	41.0	8.6	29.7	9.6	0.0	7.0	14.5	13.7	4.8	2.7	11.1	6.8	23.3	27.8	67.7	56.1
La	12.0	15.0	12.0	14.0	21.0	27.0	5.0	140.0	63.0	21.0	21.0	66.0	23.0	-	29.0	36.0	27.0	20.0	3.0	24.0	45.0	26.0	57.0	155.0	46.0
Ce	35.0	47.0	30.0	33.0	56.0	51.0	17.0	284.0	133.0	70.0	51.0	165.0	54.0	1.0	60.0	92.0	58.0	35.0	15.0	59.0	81.0	59.0	115.0	292.0	90.0
Pb	2.2	4.9	5.9	8.9	2.7	23.7	4.4	17.4	14.4	29.8	17.5	8.8	8.6	1.6	17.0	27.2	20.0	21.8	2.8	32.2	15.9	16.5	21.4	20.0	5.4
Pr	5.3	6.4	4.6	4.3	8.0	5.2	1.7	45.4	22.3	11.4	5.6	23.3	6.0	0.1	5.8	18.3	6.9	4.2	1.5	8.2	12.5	7.4	15.3	42.0	11.0
Sr	826.3	447.0	350.8	207.8	33.0	43.9	454.7	43.9	21.9	4.3	47.3	97.2	235.3	429.3	248.0	57.7	32.9	672.8	337.5	102.1	894.3	9.3	180.9	9.9	570.6
Nd	25.0	26.0	16.0	15.0	27.0	15.0	10.0	115.0	72.0	51.0	19.0	102.0	29.0	-	20.0	52.0	22.0	10.0	14.0	23.0	33.0	25.0	47.0	127.0	39.0
Zr	110.0	336.1	166.1	131.2	204.8	101.7	35.2	496.1	630.2	117.1	142.7	295.5	151.8	4.2	276.7	171.7	163.7	693.9	51.1	101.8	907.0	193.6	255.6	589.2	236.2
Sm	5.5	7.6	4.6	3.4	7.5	2.8	1.7	19.8	13.1	22.7	3.6	22.9	5.8	0.2	3.9	17.3	4.8	2.6	2.0	6.5	7.2	6.0	9.1	21.9	8.0
Eu	1.5	1.9	1.1	0.6	0.6	0.2	0.6	1.3	2.8	0.1	0.3	0.5	1.1	0.2	0.7	0.7	0.2	1.2	0.6	0.4	3.8	0.2	1.0	1.0	5.6
Dy	4.6	7.5	4.1	3.1	8.3	2.0	1.5	6.8	5.8	35.6	2.3	15.0	5.3	0.2	2.8	15.9	3.8	1.6	2.1	3.2	2.6	6.0	6.3	11.1	5.4
Y	29.7	49.8	25.4	21.6	53.9	15.2	9.8	30.1	31.1	213.9	11.7	78.6	37.4	0.3	19.4	93.2	26.6	10.0	14.3	16.8	11.9	44.9	45.6	63.9	28.9
Yb	2.5	4.0	2.7	2.5	6.0	1.6	0.9	2.4	2.9	17.8	1.1	5.2	3.2	0.1	1.7	9.1	2.7	1.5	1.3	1.3	1.3	4.5	3.9	6.0	2.1
Lu	0.4	0.6	0.4	0.4	0.9	0.2	0.1	0.3	0.5	2.3	0.2	0.7	0.5	0.0	0.3	1.3	0.4	0.3	0.2	0.2	0.2	0.7	0.6	0.9	0.3
Gd	5.1	7.7	4.3	3.1	7.5	2.5	1.7	14.6	10.0	28.6	3.0	19.5	5.6	0.2	3.4	16.2	4.2	2.1	2.1	5.1	5.3	5.9	7.8	17.5	7.4
Tb	0.8	1.2	0.7	0.5	1.3	0.3	0.3	1.5	1.2	5.7	0.4	2.9	0.9	0.0	0.5	2.7	0.7	0.3	0.3	0.7	0.6	1.0	1.1	2.2	1.0
Ho	1.0	1.6	0.9	0.7	1.8	0.4	0.3	1.2	1.1	7.5	0.4	2.8	1.1	0.0	0.6	3.2	0.8	0.4	0.5	0.6	0.5	1.3	1.3	2.2	1.0
Er	2.6	4.3	2.6	2.1	5.5	1.3	0.9	3.1	2.9	20.4	1.2	6.7	3.2	0.1	1.7	9.1	2.3	1.2	1.3	1.4	1.4	4.0	3.7	6.0	2.5

All 137 analysed samples and additional elements are displayed in supplementary **Appendix A**.

Table 3: A summary of classification and tectonic schemes applied to Arabian granitoids

Sampled Unit	Group	Terrane	Age (Ma)	I-S or A-type	Rock Type	Granite	Alkali	Fe or Mg	Timing	Setting
Makkah Suite [dm01a]	Island Arc	Jiddah	845.6	I	GD	M	CA	M	PCU	VAG-WPVZ
Shufay-yah Complex [su]	Synorogenic	Hijaz	715.4	I	T	M	CA	M	PPC	VAG-ACM/WPVZ
Jar-Salajah Complex [js]		Hijaz	693.2	I	G & GD	PA	C	M	SC	VAG-ACM/WPVZ
Al Hafoor Suite [ao85] Al Hafoor Suite [ao88]	Post-tectonic	Tathlith	636.0	I & A	AG	PA	CA	F & M	SC-PO	VAG-ACM/OA
Ibn Hashbal Suite [ih]		Asir	617.6	A	AG	M	AC	M & F	SC-PO	VAG-ACM
Wadbah Suite [wb]		Asir	615.9	A	AG	M	AC	F	SC-A	WPG-VAG-WPVZ
Ar Ruway-dah Suite [ku]		Ad Dawadimi	611.0	A	G	PA	AC	F	SC-PO	WPG-ACM
Kawr Suite [kw51p] Kawr Suite [kw42] Kawr Suite [kw43] Kawr Suite [kw14]		Asir	611.7 & 608	I & A	AG & G	P, PA & M	AC & CA	F & M	A-SC-PO	WPG/VAG-ACM
Haml Suite [hla]		Afif	608.6	Border line I & A	M	M	AC	M	SC-LO	VAG-ACM
Najirah Granite [nr]		Ad Dawadimi	607.0	A	G-AG	PA	AC	F	SC-PO	WPG-OG-ACM
Idah Suite [id]		Ha'il	605.8	Border line I & A	AG	PA	AC	F	SC-A	VAG-ACM
Al Khushaymiyah Suite [ky]		Afif	601.2	Border line I & A	M	PA	A	M	LO	VAG-ACM/OA
Mallik Granite [kg]	Anorogenic	Ad Dawadimi	599.6	S	G	PA	AC & CA	F & M	SC	VAG-ACM
Admar Suite [ad]		Hijaz	599.2	Border line I & A	S	M	A	M	LO	VAG-WPVZ
Al Bad Suite [abg]		Midyan	597.4	A	AG	PA	AC & CA	F & M	A	WPG-ACM
Al Hawiyah Suite [hwg]		Northern Asir	591.9	A	G & M	PA & M	AC & CA	F	SC-PO	WPG-ACV/WPVZ
Abanat Suite [aa]		Ha'il	585.0	A	AG	P	AC	F	A	WPG-ACM
Mardabah Complex [mr]		Hijaz	525.6	A	S	M	A	F	LO	WPG-WPVZ

Table symbols: **I-S or A-type** (Whalen et al. 1987). **Rock type** AG=Alkali-Granite, G=Granite, M=Monzonite, S=Syenite, GD=Granodiorite, T=Tonalite, D=Diorite (De la Roche et al. 1980). **Granite** P=Peralkaline, PA=Peraluminous, Metaluminous (Frost et al., 2001). **Alkali** AC=Alkali-calcic, CA=Calc-alkalic, A=Alkalic, C=Calcic (Frost et al. 2001). **Fe or Mg** F=Ferroan, M=Magnesian (Frost et al. 2001). **Timing** A=Anorogenic, SC=syn-collisional, PO=Post-Orogenic, LO=Late Orogenic, PCU=Post-Collisional Uplift, PPC=Pre Plate Collision (Batchelor and Bowden, 1985). **Setting** WPG=Within-plate Granite, VAG=Volcanic Arc Granite, OG=Orogenic Granite ACM=Active Continental Margin, WPVZ=Within-plate Volcanic Zone, OA=Oceanic Arc (Pearce et al., 1984a).

Table 4: A summary of Nd, Sm and Sr isotopes determined by TIMS for all sampled suites and associated gabbros & volcanics.

Sample	Terrane	Age (Ma)	Rock Type	Tectonic Timing	Sm (ppm)	Nd (ppm)	$^{147}Sm/^{144}Nd$	$^{143}Nd/^{144}Nd$	$^{143}Nd/^{144}Nd$ (t)	2σ	εNd	εNd(t)	DM(t) Ga	Rb (ppm)	Sr (ppm)	$^{87}Sr/^{86}Sr$	2σ	$^{87}Sr/^{86}Sr$ (t)
Shufayyah Complex [su216]	Hijaz	715.4	Tonalite	Synorogenic	3.8	17.0	0.1353	0.512653	0.512019	7.6	0.29	5.91	0.96	43	350.8	0.706177	10.4	0.703013
Jar-Salajrah Complex [js202]	Hijaz	705.9	Granodiorite	Synorogenic	3.2	16.3	0.1186	0.512582	0.512043	7.5	-1.10	5.84	0.90	26	207.8	0.706122	11.6	0.702826
Al Hafoor Suite [ao85]	Tathlith	636	Alkali-Granite	Post-orogenic	2.7	16.2	0.0991	0.512406	0.511993	13.3	-4.51	3.42	0.98	179	43.9	0.806404	12.8	0.698286
Al Hafoor Suite [MD95]	Tathlith	636	Granodiorite	Post-orogenic	1.7	11.1	0.0918	0.512403	0.512020	7.8	-4.57	3.95	0.93	69	1024	0.704789	10.6	0.703144
Ibn Hashbal Suite [ih68]	Asir	617.6	Alkali-Granite	Post-orogenic	16.6	126.9	0.0791	0.512417	0.512097	9.3	-4.30	4.99	0.83	61	32.9	0.803196	12.4	0.753914
Wadbah Suite [wb65]	Asir	615.9	Alkali-Granite	Post-orogenic	12.8	81.6	0.0952	0.512479	0.512094	8.1	-3.11	4.88	0.86	63	21.9	0.762602	10.7	0.687647
Ar Ruwaydah Suite [ku139]	Ad Dawadimi	611.0	Alkali-Granite	Post-orogenic	2.7	14.0	0.1153	0.512446	0.511984	7.5	-3.74	2.64	1.08	88	295.9	0.710556	11.6	0.702783
Kawr Suite [kw42]	Asir	611.7	Granodiorite	Post-orogenic	22.5	100.2	0.1356	0.512628	0.512085	8.0	-0.39	4.39	1.03	97	97.2	0.727509	13.2	0.701513
Kawr Suite [kw51p]	Asir	608	Alkali-Granite	Post-orogenic	3.4	18.8	0.1084	0.512532	0.512100	6.7	-2.08	4.79	0.89	110	55.2	0.760414	127	0.707887
Haml Suite [hla110]	Afif	608.6	Quartz-Monzonite	Post-orogenic	3.9	21.5	0.1086	0.512478	0.512045	7.1	-3.13	3.73	0.97	125	248.0	0.715626	12	0.702543
Najirah Granite [nr120]	Ad Dawadimi	607	Granite	Post-orogenic	15.4	61.7	0.1506	0.512630	0.512031	9.0	-0.14	3.44	1.24	182	57.7	0.779715	19.4	0.696248
Idah Suite [id159]	Ha'il	605.8	Alkali-Granite	Post-orogenic	4.7	24.8	0.1158	0.512512	0.512051	8.0	-2.46	3.83	0.99	136	43.9	0.735379	11.8	0.654438
Al Khuashaymiyah Suite [ky129]	Afif	601.2	Quartz-Monzonite	Post-orogenic	2.4	15.1	0.0974	0.512340	0.511957	7.7	-5.81	1.81	1.05	107	672.8	0.707630	10.5	0.703679
Malik Granite [kg150]	Ad Dawadimi	599.6	Granite	Anorogenic	6.2	29.0	0.1301	0.512495	0.511984	9.8	-2.78	2.33	1.18	165	102.1	0.742676	12.6	0.700113
Admar Suite [ad194]	Hijaz	599.2	Syenite	Anorogenic	6.1	42.4	0.0873	0.512428	0.512086	11.1	-4.09	4.29	0.87	41	894.3	0.703946	12	0.702819
Al Bad Suite [abg179]	Midyan	597.4	Alkali-Granite	Anorogenic	5.6	25.7	0.1317	0.512639	0.512123	8.1	0.02	4.99	0.94	159	9.3	1.089832	15.1	0.652145
Al Hawiyah Suite [hwg07]	Northern Asir	591.9	Granite	Anorogenic	8.4	47.6	0.1060	0.512520	0.512109	8.3	-2.31	4.55	0.89	200	180.9	0.729219	10.8	0.702226
Abanat Suite [aa166]	Ha'il	585*	Alkali-Granite	Anorogenic	21.1	138.6	0.0921	0.512466	0.512113	8.3	-3.35	4.47	0.85	148	9.9	0.990950	14.2	0.619404
Mardabah Complex [mr191]	Hijaz	525.6	Syenite	Anorogenic	7.6	40.6	0.1128	0.512529	0.512141	9.2	-2.13	3.51	0.93	41	570.6	0.704534	9.5	0.702662
Gabbros and Volcanics																		
Makkah Suite [dm01a]	Jiddah	845.6	Gabbro-Diorite	Island Arc	5.4	24.7	0.1336	0.512592	0.511852	11.2	-0.90	5.94	1.05	40	826.3	0.704364	10.2	0.703102
At Ta'if Group [tfv02]	Jiddah	840*	Chlorite-Schist	Island Arc	2.3	12.1	0.1151	0.512412	0.511778	7.8	-4.42	4.36	1.13	11	22.3	0.715381	25.6	0.703585
Siham Group [si116]	Afif	750*	Rhyolite	Synorogenic	9.6	56.8	0.1026	0.512211	0.511706	7.7	-8.32	0.70	1.28	185	70.5	0.772496	15.5	0.707962
Al Ays Group [ay187]	Hijaz	700*	Dacitic-Andesite	Synorogenic	2.9	11.9	0.1474	0.512724	0.512047	8.1	1.67	6.08	0.70	13	235.9	0.704543	11.2	0.703119
Subh Suite [sf209]	Hijaz	698.7	Rhyolite	Synorogenic	6.4	28.8	0.1351	0.512665	0.512047	9.5	0.53	6.04	0.93	67	33.0	0.752144	11.1	0.699021
Al Hafoor Suite [ao88]	Tathlith	636	Gabbro-Norite	Post-orogenic	1.8	7.7	0.1384	0.512530	0.511953	7.9	-2.11	2.63	1.24	16	454.7	0.704720	12.6	0.703831
Bani Ghayy Group [MCR105]	Afif	630*	Basalt	Post-orogenic	3.1	13.2	0.1420	0.512630	0.512044	8.1	-0.14	4.27	1.09	21	567.2	0.703967	11.9	0.703062
Murdama Group [mu132]	Ha'il	630*	Rhyodacite	Post-orogenic	6.2	32.3	0.1154	0.512421	0.511945	7.9	-4.22	2.33	1.12	60	885.9	0.705698	12.7	0.704010
Kawr Suite [kw43]	Asir	612	Gabbro-Diorite	Post-orogenic	5.7	25.7	0.1350	0.512477	0.511935	8.0	-3.14	1.68	1.29	0.8	235.3	0.705530	10.6	0.705447
Rithmah Complex [rt185]	Hijaz	600*	Gabbro-Diorite	Anorogenic	2.0	7.7	0.1615	0.512790	0.512156	7.9	2.97	5.67	1.03	16	337.5	0.704028	10.3	0.702784
Hadn Formation [hn160]	Ha'il	598*	Rhyodacite	Anorogenic	5.5	27.8	0.1194	0.512610	0.512142	8.0	-0.55	5.37	0.87	65	264.5	0.708841	15.5	0.702814
Mardabah Complex [CV192]	Hijaz	526	Granophyre	Anorogenic	12.9	67.8	0.1154	0.512537	0.512140	9.7	-1.97	3.49	0.94	29	506.1	0.704383	10.8	0.703145

Raw data are presented in supplementary **Appendix B**. Calculated model ages are based on ratios taken from Goldstein et al. (1984). The U-Pb ages are taken from Robinson et al. (2014) with the exception of * values which were taken from Johnson (2006).

Table 5: The subdivision parameters for Arabian Shield suites

Group Name	Suites included	Shield position	Rock type	Hypersolvus (coarse perthite)	Aegirine-bearing	Tectonic Classification
IA +Syn (~845-700 Ma)	dm, su, js	western Shield	Gabbro - Tonalite	-	-	VAG
NHSG (~640 - 610 Ma)	ao, ih, wb, ku, kw, nr	Nabitah and Halaban Suture	Gabbro - Alkali-Granite	✓	✓	VAG-WPG
POPG (~610 - 600 Ma)	hla, id, ky, rt, ad, kg	western and eastern Shield	Gabbro - Alkali-Granite	✓	-	VAG
AAPG (< 600 Ma)	abg, hwg, aa, mr	western and eastern Shield	Syenite - Alkali-Granite	✓	✓	WPG

Abbreviations IA +Syn = Island Arc and Synorogenic Granitoids, NHSG = Nabitah and Halaban Suture Granitoids, POPG = Post – Orogenic Perthitic Granitoids, AAPG = Anorogenic Aegirine Perthitic Granitoids. Note rt (~600 Ma) is placed into the POPG field due to its coeval relationship with the Admar Suite (ad) and its geochemistry. Similarly, kg (~600 Ma) is an S-type granite that intrudes the Idah Suite (id), so it is also placed into the POPG field.

Geochemical and isotopic constraints on island arc, synorogenic, post-orogenic and anorogenic granitoids in the Arabian Shield, Saudi Arabia.

F.A. Robinson[a*], J.D. Foden[a], A.S.Collins[a]

[a]Department of Earth Sciences, The University of Adelaide, SA, 5005, Australia
*Corresponding author: frank.robinson@adelaide.edu.au, 14 Johnson Road, Athelstone, SA 5076 Australia Ph +61 8 83370577
Co-author: john.foden@adelaide.edu.au, alan.collins@adelaide.edu.au

Highlights

- Geochemistry identifies 4 Arabian granitoid groups: IA+Syn, NHSG, POPG and AAPG
- Nd isotopes distinguish contamination in A-type granite sources beneath sutures
- Nb and Y suggest two ANS mantle sources: contaminated and enriched
- IA+Syn, NHSG and POPG are generated in depleted MASH zones
- Within plate AAPG are derived from enriched mantle associated with delamination